Fall 1-31-2007

Inverse dynamic modeling for characterization of spasticity

Katharine Markel Swift
New Jersey Institute of Technology

ABSTRACT

INVERSE DYNAMIC MODELING FOR CHARACTERIZATION OF SPASTICITY

by
Katharine Markel Swift

Spasticity affects subjects with cerebral palsy, stroke, multiple sclerosis, and traumatic brain injury. The need to develop a deeper understanding of spasticity is driven by the existing limited understanding and the lack of satisfactory interventions for this disabling phenomenon.

An inverse model is implemented to describe the motion in the pendulum knee drop test. Inverse kinematic modeling is implemented to investigate the pathophysiology of spasticity.

Using the equilibrium point hypothesis as a conceptual framework to explain disabled and non-disabled neuromuscular control, it has been demonstrated that the equilibrium point of the passive knee is dynamic and exhibits a pseudo-exponential trajectory in spasticity that is different from the non-spastic case. In non-spastic subjects, this research has shown that there is nonlinearity at the highest velocity of the pendulum knee drop test due to muscle activation. In spastic subjects, this research has also demonstrated that the passive linear stiffness is increased. This work now allows biomechanical variants to be linked with two important clinical concepts associated with spasticity. Increases in passive linear stiffness can be equated with increased tone in spasticity. The dynamic equilibrium point trajectory can be used to explain the hyperactive stretch reflex.

INVERSE DYNAMIC MODELING FOR CHARACTERIZATION OF SPASTICITY

by
Katharine Markel Swift

A Thesis
Submitted to the Faculty of
New Jersey Institute of Technology
in Partial Fulfillment of the Requirements for the Degree of
Master of Science in Biomedical Engineering

Department of Biomedical Engineering

January 2007

APPROVAL PAGE

INVERSE DYNAMIC MODELING FOR CHARACTERIZATION OF SPASTICITY

Katharine Markel Swift

Dr. Richard A. Foulds, Thesis Adviser — Date
Associate Professor of Biomedical Engineering, NJIT

Dr. Sergei Adamovich, Committee Member — Date
Assistant Professor of Biomedical Engineering, NJIT

Dr. Lisa K. Simone, Committee Member — Date
Assistant Research Professor of Biomedical Engineering, NJIT

BIOGRAPHICAL SKETCH

Author: Katharine Markel Swift

Degree: Master of Science

Date: January 2007

Undergraduate and Graduate Education:

- Master of Science in Biomedical Engineering,
  New Jersey Institute of Technology, Newark, NJ, 2007

- Bachelor of Science in Business and Economics,
  Lehigh University, Bethlehem, PA, 1999

Major: Biomedical Engineering

ACKNOWLEDGMENT

I wish to thank professors Richard A. Foulds, Sergei Adamovich, Lisa K. Simone, Bruno A. Mantilla for their tireless guidance and insight. It has been a great experience to learn under you. In addition I would like to thank my lab peers, specifically those involved in data collection, your friendship will remain with me forever.

I am grateful for the support from the Rehabilitative Engineering Research Center. I envision the RERC doing great things in years to come.

TABLE OF CONTENTS

TABLE OF CONTENTS
(Continued)

LIST OF FIGURES

LIST OF FIGURES
(Continued)

LIST OF FIGURES
(Continued)

CHAPTER 1

INTRODUCTION

1.1 Objective

Understanding the mechanisms of spasticity would provide a better rationale for therapeutical decisions. Since existing clinical measures of spasticity are limited in consistency and sensitivity, this understanding would also provide grounds for objective measures of results from interventions used to reduce spasticity including surgery, electrical stimulation, drugs, and physical therapy. [3]

An inverse model has been implemented to describe the motion in the pendulum knee drop test. Inverse modeling, which utilizes experimental data to derive model parameters, helps predict variables that are not directly measurable in humans. [10] Benefits from modeling include that it provides an orderly description of a problem and that it notes a benchmark for further developments to be used in the clinical setting. In the case of movement disorders, simulation of complicated pathology provides a way to understand the mechanisms of the disorder and faulty parameters. In a clinical setting such models can be used to track and quantify progression.

Utilizing complex models, various studies have attempted to explain spasticity in terms of increased muscle torque from changes in linear and nonlinear stiffness and damping. Existing research fails to correlate complex model manipulations with the pathophysiology of spasticity.

Conclusions drawn from the following model equate clinical definitions with mathematical ones. There is an increase in passive stiffness in subjects with spasticity

that equates with the clinical concept of increased tone. There is also a dynamic equilibrium point that equates with the clinical definition of hyperactive reflex. This inverse model uses experimental data from three triplets—two of whom have cerebral palsy and one who does not—and one additional non-spastic control subject. A residual torque value that includes active and passive stiffness and stretch reflex torque generates a perfect fit to experimental data in both the disabled and non-spastic subjects. To account for the changes in trajectory between spastic and non-spastic subjects it is hypothesized that spasticity is caused by changes in the equilibrium point due to stretch reflex activation. In this model the equilibrium points are the trajectory values where the residual torque is equal to zero. These are also the points where accelerations are approximately equal to zero. In the passive muscle state, the trajectory and residual torque should remain at zero and in the active state the trajectory should become non-zero to reflect muscle activation. It is assumed that in non-spastic subjects the equilibrium point is at zero because there is no reflex activation. This hypothesis is employed in experimentation on the non-spastic subject. The resultant data shows that in the first swing of the pendulum knee drop test there is a non-zero equilibrium point in non-spastic subjects, and thereafter the equilibrium point decreases to zero. By pairing EMG activity with non-zero equilibrium points this research offers a hypothesis that there is muscle activation in early swing of the non-spastic trajectory. Thus, the research on spasticity has additionally led to a characterization of well-known nonlinearity in non-spastic subjects.

CHAPTER 2

BACKGROUND

2.1 Spasticity

This research is focused on a study of spasticity that results from neural damage. "Spasticity is a motor disorder characterized by a velocity-dependent increase in tonic stretch reflexes (muscle tone) with exaggerated tendon jerks, resulting from hyper-excitability of the stretch reflex, as one component of the upper motor neuron syndrome." [11]

Spasticity affects subjects with a variety of conditions such as cerebral palsy, stroke, multiple sclerosis, and traumatic brain injury. It is co-morbid with impaired motor function, but the extent to which it actually causes motor loss is debated in the literature. In extreme cases spasticity can lead to paresis. Other symptoms of spasticity include hypertonia (resistance to passive stretch), spasms, and loss of sensory function. [12] Reduction of spasticity decreases abnormally high muscle tone, inappropriate co-contraction, and hyperactive reflexes and can improve the quality of life by enhancing ambulation and upper extremity function.

2.1.1 Neural Basis of Spasticity

Due to the complexity of the central nervous system, the exact process involved in spasticity is still unknown. [5] Stretch reflex, as exhibited by a tendon tap, is believed to be a major component causing spasticity. The torque generated in muscle activation is a monosynaptic reflex that is generated by feedback to the alpha motor neurons. The

mechanism is believed to start at the muscle spindle, which reacts to change in length and velocity. Muscle spindle activation excites Ia afferents that in turn excite the alpha motor neurons that innervate the muscle. [8]

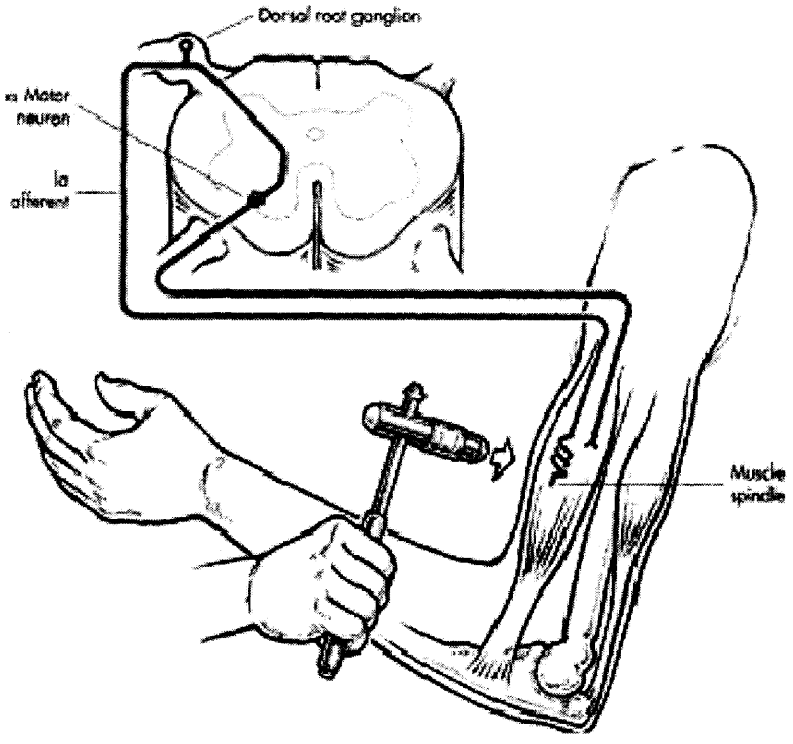

Figure 2.1: Stretch reflex circuit.
(Source: C. T. Leonard, *The Neuroscience of Human Movement*, 1998.)

While the stretch reflex is monosynaptic, it branches off to other areas that convey inhibitory information. Inhibitory pathways involved include Ia inhibition, Ib inhibition, Renshaw cells, and presynaptic inhibition. Ia inhibitors secrete neurotransmitters to inhibit antagonist muscle innervation. Under descending control from the brain, Renshaw cells project to alpha motor neurons and inhibitory Ia interneurons. Activation of Renshaw cells inhibits alpha motor neurons and gamma motor neurons (control the sensitivity of muscle spindles in contraction), in addition to Ia inhibitory interneurons. Renshaw cells inhibit alpha motor neurons, which also cause alpha motor neuron

activation. They are thought of as "variable gain regulators" by inhibiting agonist muscles and disinhibiting (reducing inhibition) antagonist muscles. [22]

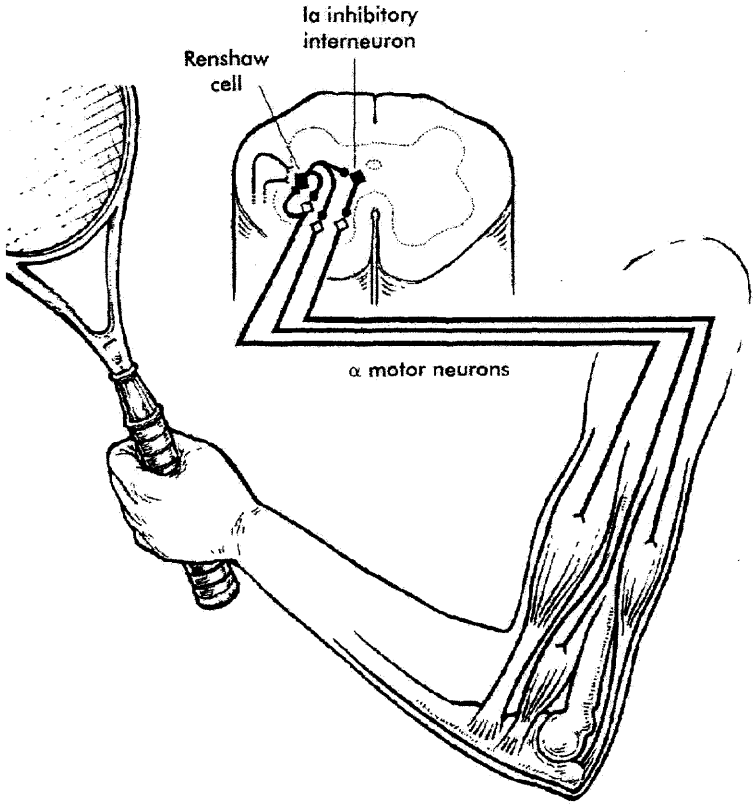

Figure 2.2: Inhibitory pathways.
(Source: C. T. Leonard, *The Neuroscience of Human Movement*, 1998.)

The stretch reflex activation threshold is modulated by descending neural signals. While the precise mechanism is not fully understood, it is believed that neural damage can alter the descending signals, drastically altering (lowering) the reflex threshold. This lowered threshold is a prime contributor to spasticity. [22]

2.1.2 Dysfunctional Causes of Spasticity

Spastic impairment results from a combination of changes in muscle characteristics and in the brain, caused by damage to the pathways from the cerebral cortex to the brain stem and spinal cord. [22] There are two kinds of spasticity, one that results from brain damage as in the case of cerebral palsy, multiple sclerosis, stroke, and traumatic brain injury, and the other that results from spinal cord injury. This research is limited to spasticity resulting from brain damage.

In the brain several pathways are effectively causing the disability. There are many theories but no final definition of what the main contributor of spasticity is. For example, one theory states that there is increased gamma motor neuron activity. [8] Another is that muscle spindle sensing is more complex than fully understood, and is increased significantly in spasticity. [4] There is also speculation that there are deficient inhibitory factors, specifically deficient reciprocal Ia inhibition. [8] Spasticity has also been attributed to dysfunctional mechanisms at the supraspinal level that block unnecessary afferent inputs, causing threshold to be lowered, and allowing stretch reflex activation to occur more often. [22] Finally, there could be high levels of Renshaw cell activation causing spasticity that result in excessive muscle co-contraction from inability to grade muscle forces. [22]

In spasticity, changes in muscle characteristics are also believed to be dysfunctional. Muscle characteristics include intrinsic stiffness and damping, which account for a number of components in a human joint from the passive properties of muscle fibers and connective tissue. [3] Some of the passive elastic tissues include tendons, fascia, ligaments, joint capsules, skin, cartilage, and inactive muscles. The joint

is also viscous, creating a damping force, from passive tissue interaction among interstitial fluid, protoplasm, synovial fluid, joint capsule, and skin. [17] These passive forces are changed in spasticity, but like in the case of the central nervous system, there is no clear understanding of what and how the muscle is changed. The main theory for changes in passive stiffness and damping is that they are due to long-term changes in muscle fiber over time from immobility. Neilsen *et al.* cite studies where passive stiffness is increased by 400% in patients with damage to central motor pathways. [8] Yet, Fee *et al.* have clearly indicated that following experimental vestibular stimulation, subjects with cerebral palsy exhibit marked changes in spasticity. They have shown that these changes in passive joint stiffness and damping, as well as the reflex threshold in spastic subjects, are even more significantly attenuated following anesthesia. Their research argues against changes in tissue characteristics as a major cause of spasticity. [26] Finally, the use of medication argues against changes in the material structure of muscle being causal, since spastic improvement is seen within minutes of administering the drug.

2.1.3 Interventions

Existing interventions for spasticity are drastic. They include surgery, electrical stimulation, drugs, and physical therapy. [3]

The majority of spastic subjects take drugs to reduce the spasticity. Medication like baclofen and diazepam increase presynaptic and postsynaptic inhibition, decreasing the excitability of the motor neuron. It is an imperfect intervention because it also depresses voluntary excitation, as evidenced by the increase in postsynaptic inhabitation.

The future of antispastic medication is to develop a drug that depresses stretch reflex excitation while not affecting excitation coming from the descending pathway. [8]

2.1.4 Measures of Spasticity

Existing measures of spasticity are limited in consistency and sensitivity. Current measures fail to quantify the underlying mechanisms, severity, and impairment to the subject.

2.1.4.1 Ashworth Scale. The most widely used measure of spasticity in the clinical setting is called the Ashworth scale. The Ashworth scale is a qualitative numeric scale—from 0 to 4—that measures the resistance to stretch. The major limitation of the Ashworth scale is the lack of sensitivity to changes. [13] Nordmark and Andersson suggest that the Ashworth scale "suffers from the clustering effect with most patients grouped in the middle grades." Attempts to solve this problem have resulted in adding another grade. The new scale, consisting of 6 points (0, 1, 1+, 2, 3, 4) and called the Modified Ashworth scale, is still not ideal because it cannot differentiate types of tone and relies too heavily on the practitioner's discernment of the spasticity. [7]

2.1.4.2 Pendulum Knee Drop Test. The pendulum knee drop test was first documented by Wartenberg as a measure to quantify hypertonia in Parkinson's disease. Since then it has been used mainly in the research setting to assess changes in tone resulting from many other neurological diseases. [7] Some benefits of the test are that it is quick and easy, non-invasive, and reliable. It is also specific to the quadriceps, which is an important muscle in motor activity. Most important, the pendulum test is best in subjects with cerebral palsy because it is easy to administer. [13]

The pendulum knee drop uses gravity in passive swing to provoke muscle stretch reflexes. During the test the subject is seated or supine with his or her leg extended. Different positions do not seem to matter. Brown evaluated the importance of position and found that it created little variability. [7] The test initiates when the leg is released and allowed to fall freely. In the decent to zero velocity, the leg typically exhibits several pendulum oscillations of decreasing movement. [7]

The major changes in spasticity are revealed from a plot of the trajectory of the leg during the pendulum knee drop test. Fowler *et al.* noted characteristics of the plot of the pendulum knee drop test and evaluated the correlation to spasticity. The characteristics included number of oscillations, duration of oscillations, amplitude of the first backward swing, and relaxation index—defined as the magnitude of the first backward swing divided by the difference between the starting and resting angles. The number of oscillations differs greatly between those that have the disability and those that do not. [13]

It is argued that the pendulum test is not a fair representation of spasticity or pathological conditions. He *et al.* argue that the pendulum test is not as accurate as it could be. They state that the inherent swing of the leg is not in one plane as the test assumes. They also argue that it cannot be a fair representation since it does not take into account the descending control—since the subject is asked to relax so that only passive parameters exist, and thus supraspinal influences are held constant. Finally, they argue that there is no correlation to the subject's functional capability in the pendulum knee drop test. [5]

In direct contrast, Nordmark and Andersson found that the Wartenberg pendulum test is reliable on children. The measurements of spasticity were the amplitude of the first swing divided by the amplitude of the final position, the amplitude of the first swing divided by the amplitude of the rebound angle, maximum velocity, and the time between the peaks. They found a strong correlation between swing time and height in non-spastic subjects. They believed that swing time was the most reliable and sensitive variable. Amplitude of the first swing divided by the amplitude of final position was an indicator of the quadriceps reflex. [7]

The pendulum knee drop test does have its limitations, but its ease of use makes it attractive for use on children with disabilities. This test also allows us to isolate the spastic torque input that is causing the disability. It is important to note that the test is not a clinical means to an end, but instead, a means to better understand, select, and evaluate future clinical measures.

2.2 Use of Models

Models help us understand underlying mechanisms of movement. Inverse modeling, which utilizes experimental data in the model parameters, helps predict variables that are not directly measurable in humans. [10] Benefits from modeling include that it provides an orderly description of a problem and that it determines a benchmark for further developments to be used in the clinical setting. In the case of movement disorders, simulation of complicated pathology provides a way to understand the mechanisms of the disorder and dysfunctional parameters. In a clinical setting, models can be used to track and quantify progression. Limitations of the Ashworth scale necessitate new tangible and

quantifiable measures, such as stiffness, to be used a in healthcare setting that is increasingly dependent on confirming interventions viable to managed care providers.

Winter states that if we have a "full kinematic description, accurate anthropometric measures and the external forces, we can calculate joint reaction forces and muscle moments." Winter goes on to state that the key to a model is the measure of accuracy of the above data. [10]

There is an inherent problem of estimation in all biomechanical models. Parameters including segment masses and lengths, damping, stiffness, and moment of inertia are all estimates that cannot be directly measurable. Winter states that at the extreme range of joint movement, passive structures such as elasticity or viscosity add or subtract from the net moment. He concludes by stating that "unless the muscle is silent, it is impossible to determine the contribution of these passive structures." In conclusion, all models must make assumptions, but ideally these assumptions should be minimal and relate to the biological component they simulate.

2.2.1 Pendulum Knee Drop Model

The equation to describe the pendulum knee drop test has many variants, but the widely used formula is the equation developed by Badj, Vodovnik, and Bowman: $I\theta'' + B\theta' + K\theta = mgl\sin\theta$ where I is the moment of inertia, θ'' is angular acceleration, B is the damping coefficient, θ' is angular velocity, K is the stiffness coefficient, θ is trajectory of the knee joint, m is segment mass (defined as the mass of the modeled limb, in this case the leg and foot), g is gravity, and l is segment length (defined as the length of the leg and foot).

2.3 Literature Review of Alternative Hypotheses

2.3.1 Threshold and Gain

Various scientific papers propose that spasticity is due to changes in threshold and gain at the muscle spindle level. Threshold is the point at which motor neuron excitability elicits muscle contraction. The belief is that in spasticity this threshold is decreased. Gain refers to the intrinsic baseline torque from stiffness in muscles, joints, and tendons. In spasticity the belief is that this gain is increased.

Schmit *et al.* modeled reflex torque response in the elbow of eight hemiparetic brain-injured subjects. They concluded that the two components of reflex response were angular threshold and reflex stiffness, where reflex stiffness was the slope of the torque versus angle plot, and angular threshold was the intercept. [25] Biologically speaking, angular threshold is defined as the angle when the passive muscle shows motor neuron activation. [6] Jobin and Levin proposed that stretch reflex threshold indicates the level of spasticity and the level of deficient motor control. [16] Powers *et al.* noted that changes in trajectory and stiffness due to spasticity are from changes in stretch reflex threshold. [25] Finally, Jobin *et. al.* cites Levin, Fel'dman, and Dimov who noted that threshold is inversely correlated with the level of spasticity and positively correlated with residual motor function in the impaired limb. [16] They proposed that the central nervous system may regulate the threshold angle in addition to the muscle force.

The concept of threshold and gain attempts to describe all of the torque in the model. It does not disassociate itself from the baseline torque that exists in a non-spastic

subject. This makes it difficult to locate what mechanisms are dysfunctional since there is no comparison to the control, non-spastic subject. Further proving this point, Jobin and Levin question whether we can accurately characterize the stretch reflex as being the result of changes between the threshold or gain. [16]

2.3.2 Spastic (Residual) Torque Isolation

Theoretically speaking, in non-spastic subjects residual torque equals all passive elastic torque. In spastic, disabled subjects the residual torque represents all passive elastic, active elastic (caused by higher muscle activation), and dysfunctional reflex torques. Attempts to isolate reflex and passive torques do not point to reflex as the only influence in spasticity. Instead, it is a combination of changes in passive and reflex torque activation that cause a limb to become spastic. Again, there is no way to measure reflex and passive torques, so assumptions have to be made to isolate the two. The following is a review of how to isolate residual torque, how to separate passive elastic from reflex, and how to calculate a value for stiffness from the measure of passive elastic torque.

Many studies note the problem of separating reflex from passive torque. Nielsen *et al.* argue that there are no agreed-upon conclusions for how to isolate residual torque since the resistance to passive stretch in the pendulum test is not only from reflex torque but also from passive elastic torque. Mirbagheri *et al.* confirm that there is a lack of tools to separate out reflex torque from intrinsic (passive elastic). [3]

One of the common methods used to isolate passive torque from reflex is to measure torque at very slow velocity. The resultant passive torque is created under the assumption that slow velocity cannot elicit reflex activation. Lin and Rymer identified

the minimum velocity to evoke a stretch reflex as being 5-193 degrees/sec, depending on spasticity severity. [15] Schmit *et al.* conducted elbow perturbations at a slow constant velocity to isolate passive torque. They defined passive torque as the torque at slow velocity (defined as 6 degrees/second) and singled out reflex torque by subtracting passive torque in another elbow perturbation trial. [6] This method makes a broad assumption that the experiment to isolate the passive torque and the subsequent experiment that elicits a stretch reflex contraction are the same.

Another technique to separate reflex from passive torque is to use electromyogram (EMG) recordings as an indicator of reflex activation. Attempts have also been made to simulate the behavior of the torque by inputting a torque at areas of increased EMG. Badj and Bowman used a torque function to represent the spastic limb based on EMG activity. [15]

While EMG can confirm uncontrolled muscle activation in spasticity, the question of how much the muscle activity changes the trajectory (via residual torque input) is explicitly unknown. Thus, while the timing of torque may be based on EMG activity, assumptions have to be made with regard to the magnitude of residual torque input.

2.3.3 Use of EMG

EMG activity reveals a great deal about muscle and neural activation in movement. EMG can measure voluntary, stimulated, or reflex contractions. [1] Inherently, EMG also has the ability to give information about which muscle is involved in movement. [10] In control subjects EMG is often used in conjunction with the experiment to verify that there is only passive action. In spastic subjects EMG is used to indicate dysfunctional muscle

activation. Since EMG activity can indicate that the muscles are activated, many models use the timing of EMG activity to simulate the stretch reflex activation.

Many scientific papers note other characteristics from EMG activity. Fowler *et al.* noted that EMG activity was observed during muscle lengthening. [13] They also made the correlation that the mean number of oscillations decreased with increased muscle tone. [13] Lin and Rymer also found that in spasticity the amount of flexion and number of oscillations is decreased, in addition to an increase in EMG activity. Lin and Rymer found that in spasticity EMG activity was much greater in the quadriceps than in the hamstrings. They noted that the duration of EMG increases linearly with increasing velocity. Lin and Rymer also noticed that the onset of acceleration occurs much sooner on the spastic side of hemiplegic subject versus the non-spastic side, presumably due to muscle activation evident in EMG activity. Co-contraction of the quadriceps and hamstrings as evident in EMG recordings also occurs in spasticity, and could account for deviations in stiffness and damping. [15]

2.3.4 Variants of the Badj, Vodovnik, and Bowman Equation

There are alternative ways to measure all of the coefficients in the Badj, Vodovnik, and Bowman model, $I\theta'' + B\theta' + K\theta = mgl\sin\theta$. The models discussed below address alternative methods for calculating the coefficients in the Badj, Vodovnik, and Bowman equation.

2.3.4.1 Stiffness and Damping. There are a wide range of methods used to calculate stiffness and damping. Simplicity and clear correlation to biomechanical functions are major goals of a good model. It is simple to fit a torque to a differential equation, but

what does it mean in terms of the biomechanical function? For example, Nordez *et al.* fit reflex and passive stiffness as a third-order and second-order differential equation, respectively. [21] While a good fit is important, this research suggests that without a basis for function a fit provides little use for understanding.

He *et al.* attempted to simulate muscle behavior by creating a muscle model for the stiffness term. This model approximates the elastic properties of muscle and tendon. They found that at low forces—measured in length—the stiffness was exponential. At high forces the stiffness was linear. [5]

There are many publications that suggest that stiffness and damping change with flexion and extension. Fee and Foulds found that there is a different spring and damper in flexion and extension. They propose a piecewise model for these two components driven by velocity feedback. [9]

Fee and Foulds optimized spring and damper by adjusting timing and amplitudes in a linear stepwise fashion. The belief is that the velocity-dependent signal from muscle spindle increases to a threshold point. At threshold the muscle is triggered to become active as observed in EMG. [9]

Lin and Rymer believe that K and B could be "dependent on motion amplitude, velocity, or direction of swing." They cite Lakie *et al.*, who observed that the period of resonance frequency in oscillation of the wrist as a linear function of applied torque. [14] They believe that in the pendulum test the torque is proportional to the amplitude. Referring back to the stiffness equation, the stiffness should be inversely proportional to the square of the amplitude. Their K is calculated to be the inverse square of the angular amplitude in each half-cycle. [15]

Lin and Rymer state that it is "well known" that K and B increase when muscles are active as in the case of spasticity. [24] In elbow joints stiffness was approximated in a stepwise fashion using the least squares model fit. [25] They start with the stiffness and damping of the non-spastic limb and implement a gain function that is initiated by EMG activity to describe stiffness and damping in a spastic subject. This trial found that this gain increase cannot fully explain the spastic trajectory and that EMG and spastic torque are not proportional or linear. They do, however, state that the linear relationship to EMG is a "basis to estimate a difficult parameter." They believe that this proves that there is an active muscle component in spastic torque. [15]

Nielsen *et al.* also suggested that there may be inherent altered muscle properties as a result of spasticity. [8] In biomechanics passive muscle properties are described as viscoelastic properties and exhibited by the damping coefficient. The idea is that viscoelastic properties are part of inherent muscle characteristics. [7] The observed pendulum knee drop plot of a spastic subject appears over-damped. Thus, the correlation is formed between the over-damped plot and dysfunctional viscoelastic properties.

Stein *et al.* cite many papers that argue that viscosity will be increased in spasticity. [1] Le Cavorzin *et al.* also observed what they believed to be increased viscosity in spastic subjects. [4] Validating this belief is Stein *et al.*, who say that viscosity increases with muscular contraction. [2]

2.3.4.2 Segment Mass and Segment Length. Anthropometric tables are not ideal, specifically in children with cerebral palsy. The anthropometric tables were generated using an adult cadaver; therefore, the ratio may not apply to children, whose bodies exhibit a growing and often disproportionate shape. Additionally, in disease,

muscles may be atrophic, which again causes a nonstandard body shape for which a table cannot account. [1]

Lin and Rymer did not use anthropometric tables and instead used the following calculations. They implemented a Vodovnik and Badj assumption that the leg can be approximated as a cylinder. Thus the segment length of the leg is l/2 where l is the total length. [15]

2.3.4.3 Moment of Inertia. Stein *et al.* state that there are a variety of different schemes to calculate the moment of inertia, but that the values of I across the methods "vary considerably." [1] Moment of inertia can be calculated from very complicated calculations using the distributions of masses across the segments. Masses can be obtained from cadavers, photographs, or medical imaging. [1]

Lin and Rymer calculated moment of inertia from pendulum knee drop tests where weights were added onto the subject's ankle. Knowledge of the inertia after the weights were added along with other parameters, including damping ratio and natural frequency, allowed for an estimate of the initial moment of inertia to be made using the following equation: $I = y/r_1r_2 - 1$ where y is the added inertia, r_1 is the ratio of natural frequency to added weight, and r_2 is the damping ratio to added weight. Using this method the authors state that the values were within 20% of anthropometric tables. In their model, estimates for mass were generated using anthropometric equations from Zatsiorsky and Winter. [15]

CHAPTER 3

METHODS

3.1 Subjects

This research has modeled the behavior of non-spastic and disabled subjects. The historical data was provided by James Fee from the A. I. Dupont Hospital for Children. The subjects are identical triplets, of whom two have cerebral palsy and one does not. This allows us to make the assumption of inertial and anthropometric similarity. [9] The non-spastic subject defined the model parameters for his disabled brothers. The model therefore shows that spasticity is additive to the model of the non-spastic subject. The three triplets were 9-year-old males with a mean height 1.40 ± 0.02 m and weight 27.8 ± 0.3 kg.

In addition, a secondary experiment on a control non-spastic subject was developed based on insights from the above experimental data from the triplets. The following experiment on a female 25-year-old subject sought to show that there is non-linearity in the first swing of the pendulum knee drop test that could be due to muscle activation. *(IRB Protocol Number: F04-04)*

3.2 Model

This model adheres to Newton's second law of motion, with respect to rotation where the sum of the moments equals the moment of inertia multiplied by angular acceleration.

The model isolates three moments affecting the total rotation about the knee being

gravitational, stiffness, and damping moments. The model formula is $Mg + Mr + Md = I\alpha$ where $Md = B\theta'$, $Mr = K(\theta - \theta_0)$, and $Mg = mgl\sin\theta$. With some differences, the equation developed by Badj, Vodovnik, and Bowman ($I\theta'' + B\theta' + K\theta = mgl\sin\theta$) is a rewritten equation of the above derivation. While this model has correlations to the Badj, Vodovnik, and Bowman equation, however, the reality is that joint rotation has nonlinearity unaccounted for in their model. This model adds necessary complexity to explain nonlinear behavior.

3.2.1 Characteristics of the Model

The following two components of the model are considered the novel characteristics. Passive elastic stiffness is represented as K in the stiffness moment, shown as the slope of the residual moment versus trajectory, and increased in spasticity. This model demonstrates the increase in slope of the residual torque versus trajectory between the spastic and non-spastic subject. This model contends that the increase in K is equated with the clinical concept of increased tone. Using the correlation of muscle to non-linear spring, a equilibrium point or equilibrium point is implemented into the stiffness moment. This research shows that the equilibrium point accounts for the change in trajectory when there is muscle activation. In spasticity, this is clinically represented as the hyper-activation of the stretch reflex.

3.2.1.1 Passive Elastic Stiffness. Many studies note the complexity of the stiffness component as being comprised of linear and nonlinear elastic components. Existing research has sought to mathematically model the nonlinear behavior, but since it cannot be measured the mechanism is still not completely defined. This research

demonstrates that passive joint stiffness represented by the slope of the residual torque versus trajectory plot is increased in spasticity. It also provides a basis for the non-linearity in early swing, as being from muscle activation in spastic and non-spastic subjects.

In a graph of trajectory versus residual torque, nonlinear elastic stiffness exists at the outliers. The linear region represents the most central area and accounts for passive joint stiffness.

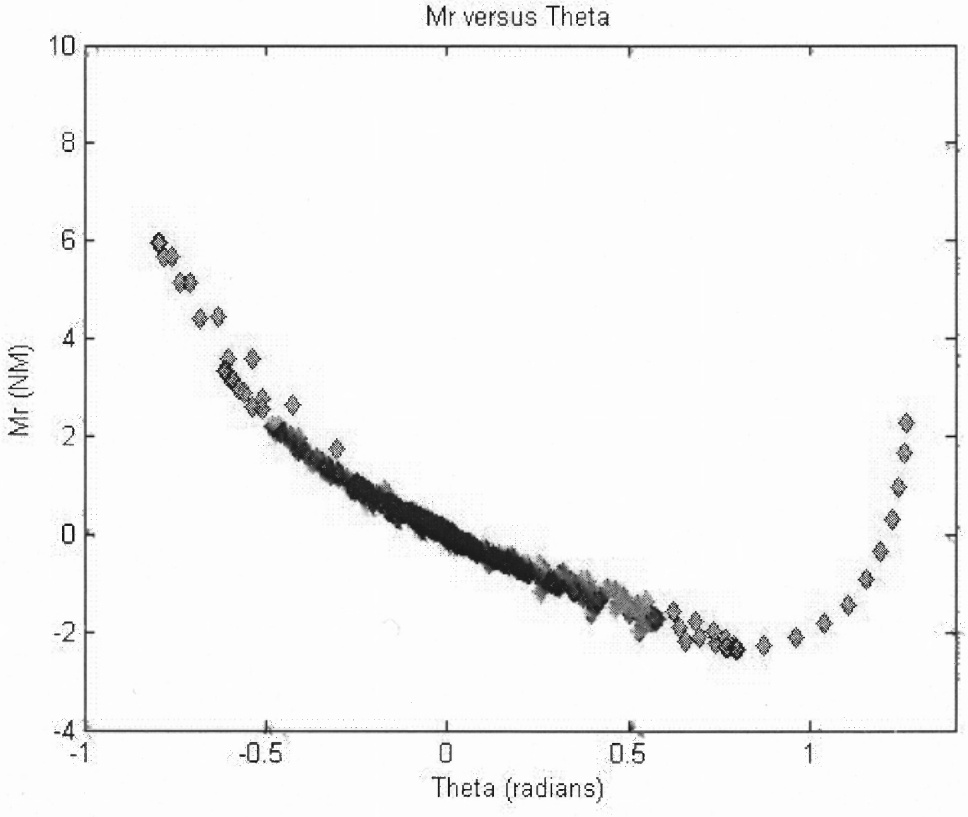

Figure 3.1: Plot of trajectory versus residual torque for the non-spastic triplet.

Passive joint stiffness is assumed to account for a number of components in a human joint. The components could be from the activation of muscle fibers and connective tissue. [3] Some of the passive elastic tissues include tendons, fascia,

ligaments, joint capsules, skin, cartilage, and inactive muscles. [17] Motion causes tendons, ligaments, skin, and inactive muscles to be deformed. The deformation causes stiffness around a joint.

3.2.1.2 Equilibrium Point. Equilibrium point is the state where forces acting on a system are at rest. In this model it is represented by the trajectory when the residual, M*r*, torque is equal to zero.

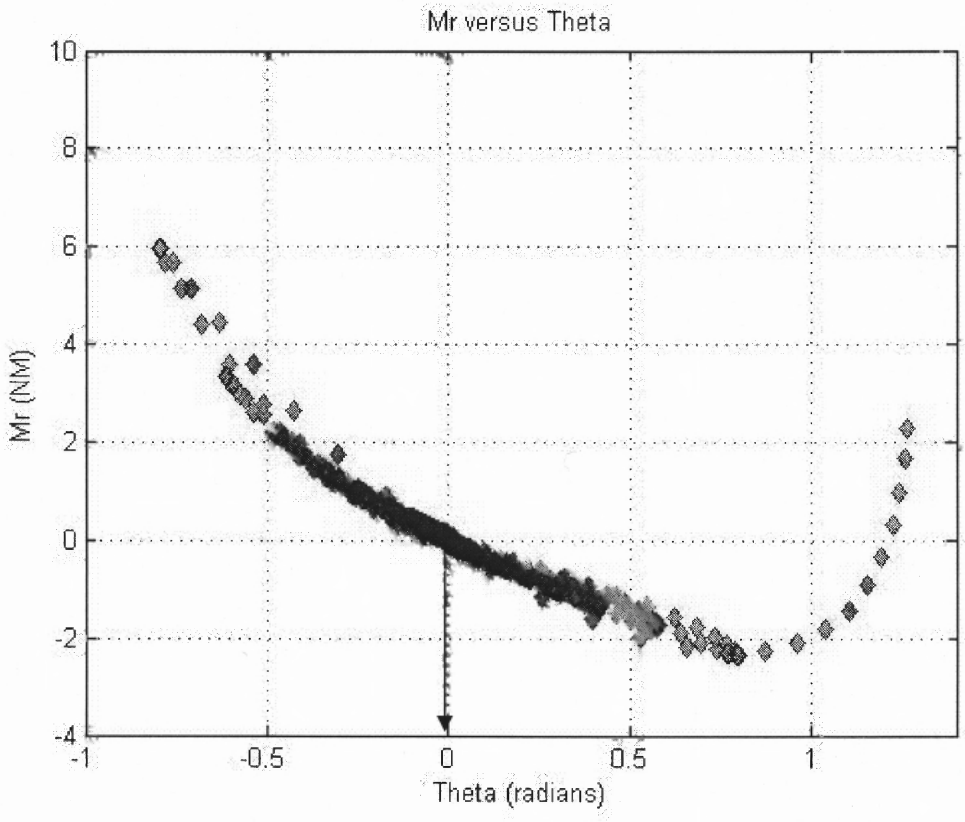

Figure 3.2: Plot of trajectory versus residual torque, M*r*, for the non-spastic triplet. Equilibrium points for the non-spastic triplets are generally at or close to zero.

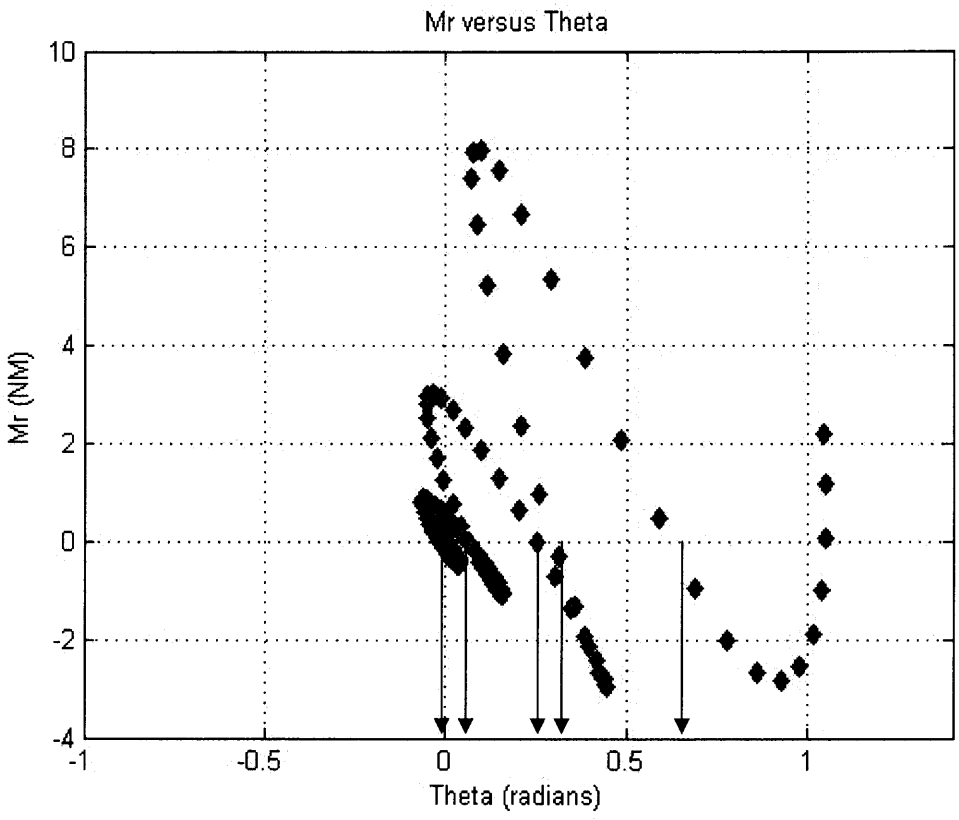

Figure 3.3: Plot of trajectory versus residual torque for the one of the spastic triplets. Equilibrium points for the spastic triplet generally do not oscillate about zero.

The equilibrium point hypothesis, developed by Fel'dman *et al.*, states that there is a threshold length, lambda, regulated by the nervous system, dynamic throughout movement, that when exceeded produces force and movement. While there are other factors that contribute to the equilibrium point calculation, generally, the point at which movement is initiated is called the equilibrium point. [23]

Fel'dman *et al.* correlated the arm muscle with the characteristics of a nonlinear spring. More specifically, he suggested that a muscle system has a static behavior that resembles a nonlinear spring with an adjustable threshold length, lambda. In the case of a stretch reflex, the point of muscle activation is where threshold length is exceeded by

actual muscle length. The result is reflex force generation, evidenced by EMG. Interestingly, Flash in 1987 showed that by shifting the equilibrium point (θ^*) the trajectory can be predicted. She used the equation $Fc = K(\theta - \theta^*) + B\theta'$, where Fc is the force generated, and shifted θ^* to create a desired trajectory. [23]

Our model implements this equilibrium point hypothesis. Since in spasticity muscles are active, there is a significant change in equilibrium point. This accounts for the fact that when the residual torque equals zero, the trajectory value is non-zero in spastic subjects. In this model, the K term is changed from $K\theta$ to $K(\theta - \theta_0)$ where θ_0 is the time-varying equilibrium point. The time-varying aspect of the equilibrium point follows the hypothesis that contraction is not a step change and instead a gradual increase or decrease in activation. [15]

By applying a time-varying equilibrium point curve this model accounts for trajectory and nonlinearities evident in both spastic and non-spastic subjects. Clinically, these changes in equilibrium points can be described as the point where there is activation of the stretch reflex.

3.2.2 Model Components

This research uses MATLAB (Math Works, Inc., Natick, MA) to implement an equation to describe the muscles intrinsic properties and extrinsic forces acting on the knee joint during the pendulum knee drop test.

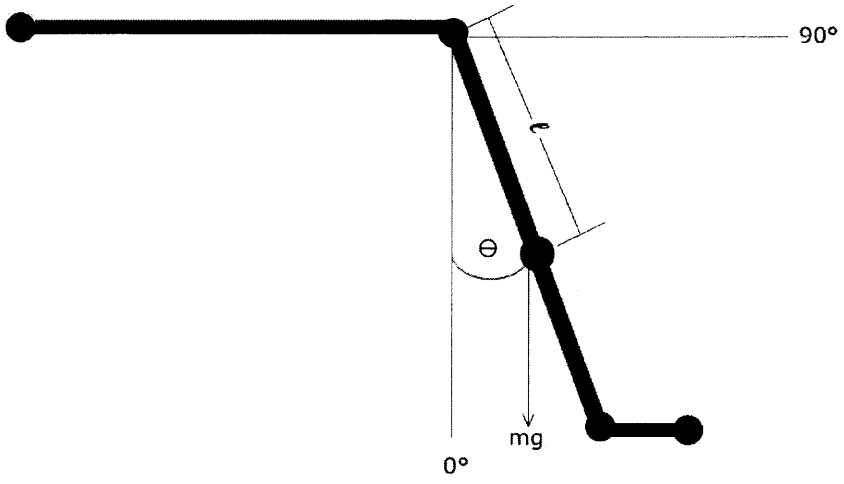

Figure 3.4: Diagram of the leg.

This model adheres to Newton's second law of motion, which holds that the rate of change of the body is directly proportional to the net forces acting on it. The linear formula for Newton's second law is: $\sum F = ma$. In the case of the pendulum test, the movement is rotational. Angular acceleration, α, is used to account for rotational movement. The moment about a rotational axis can include gravitational, external, and internal forces. Inertia, I, is the proportion that the segment resists velocity changes. [10] With rotation accounted for, the formula becomes: $\sum M = I\alpha$

This model isolates three moments affecting the total rotation about the knee: gravitational (Mg), stiffness (Mr), and damping (Md). The forces that cause moments are referred to as either external or internal forces. External forces include forces from the opposing ground force or external loads. They could be active in the case of something that is actively opposing the force, such as a person, or passive such as wind resistance.

Internal forces are the net moment of both agonist and antagonist muscles and ligament forces at all joints. [10]

Anthropometric tables are used to calculate moment of inertia, segment mass, and segment length. In 1955, Dempster *et al.* generated anthropometric tables that estimated segment lengths and joint center locations based on measurements and weights of segments taken from seven cadavers.

3.2.2.1 Moment of Inertia Multiplied by Angular Acceleration. Moment of inertia, I, is calculated using anthropometric tables. Angular acceleration, α, is calculated by taking the second derivative of the experimental trajectory data.

By using the anthropometric tables, the moment of inertia is a crude estimate. Our decision to use these tables instead of other methods was made for the sake of ease.

3.2.2.2 Gravitational Moment. The gravitational moment is located at the center of segment mass. Since it is the tangent of the rotation and relative to the axis of rotation it is represented as: $Mg = mgl\sin\theta$, where gravity is g, m is segment mass, l is segment length at the center of mass, and θ is the trajectory of the rotation.

Gravitational torque is the major component of all the moments. Stein *et al.* describe total stiffness as being equal to stiffness from gravity plus stiffness from the knee joint where gravity occupies 78% of the total. [1]

3.2.2.3 Damping Moment. It is widely believed that the damping moment describes the viscosity of the knee joint. B is the damping constant and θ' is the angular velocity of the knee joint, calculated by taking the first derivative of the experimental trajectory data.

Stein *et al.* state that the damping coefficient is the smallest and most difficult to measure accurately. [1] In attempts to limit the amount of unknowns this hypothesis

assumes that damping is linear. With a Simulink (Math Works, Inc., Natick, MA) model of our components, through trial and error, the simulation is matched with experimental data of the non-spastic subjects. Note that the model does not have a residual moment value. This value is obtained only after calculation of the above values, M*g*, M*d*, and Iα.

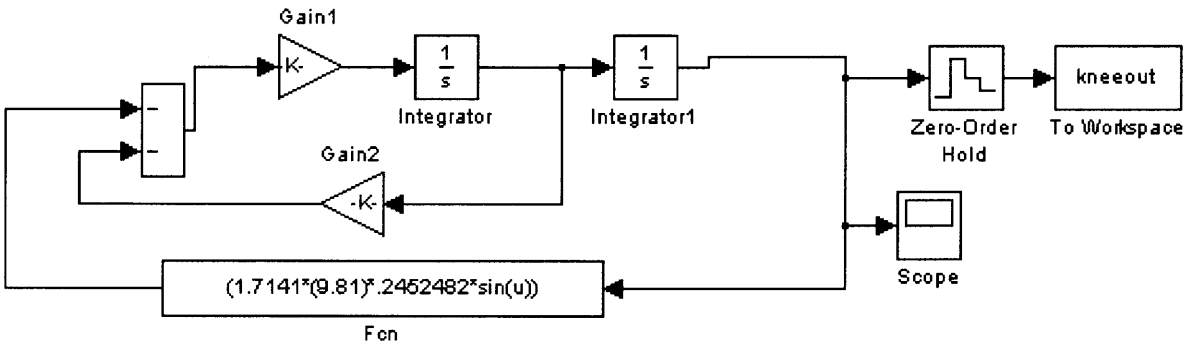

Figure 3.5: Simulink model of the pendulum knee drop.

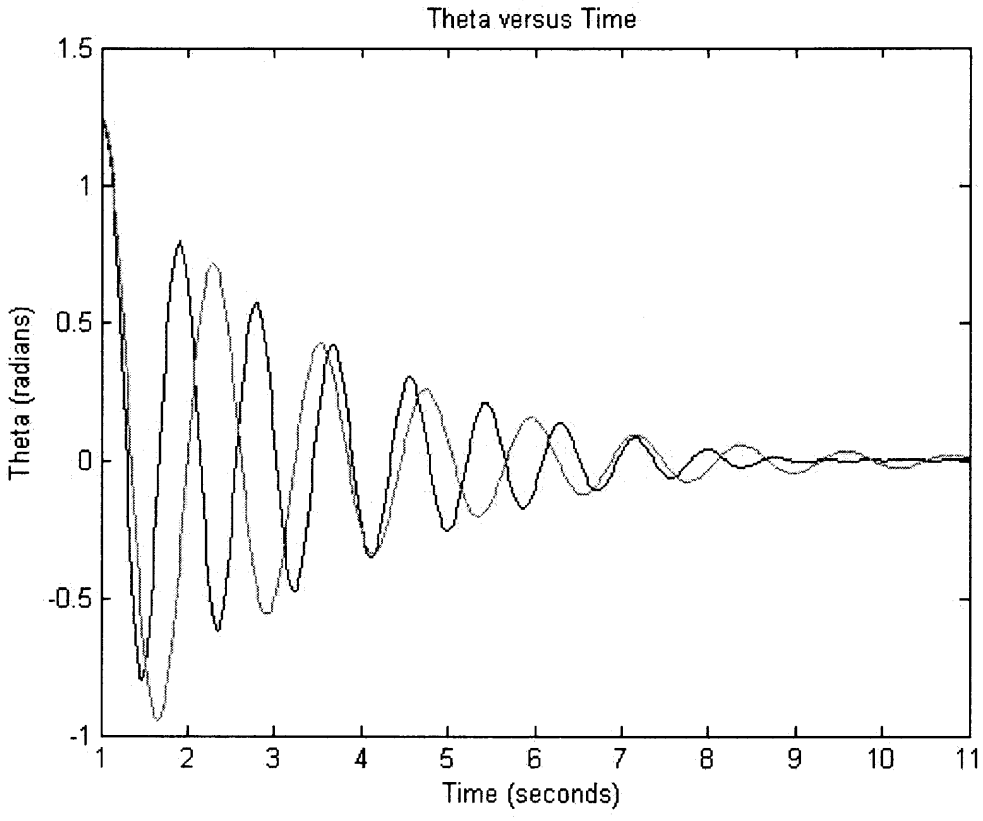

Figure 3.6: Graph of the experimental and simulated trajectory.

Differences in the two graphs can be explained by residual moment value, M*r*. Note the similarity in amplitude between the two graphs. The similarity is a good fit for the damping coefficient in the model.

3.2.2.3 Residual Moment. M*r* represents all residual moments. This hypothesis assumes it to be largely the result of joint stiffness, K (θ - θ_0), where K equals the joint stiffness and θ_0 is the equilibrium point. Note that inherently due to the way M*r* is computed, it will contain any error from estimated parameters and anonymous factors.

With experimental and calculated values for M*g*, M*d*, and Iα, M*r* is calculated by the following formula: M*r* = M*g* + M*d* + Iα. This serves to isolate all unexplained residual torque.

Equilibrium points are defined as the points where $Mr = K(\theta - \theta_0) = 0$. Since it is assumed that there is no muscle activation for non-spastic subjects, Mr equal to zero should occur twice in each pendulum swing at approximately θ equal to zero. For the subjects with spasticity, Mr equal to zero will occur at θ angles that differ in each swing. Another illustration of this method is shown below.

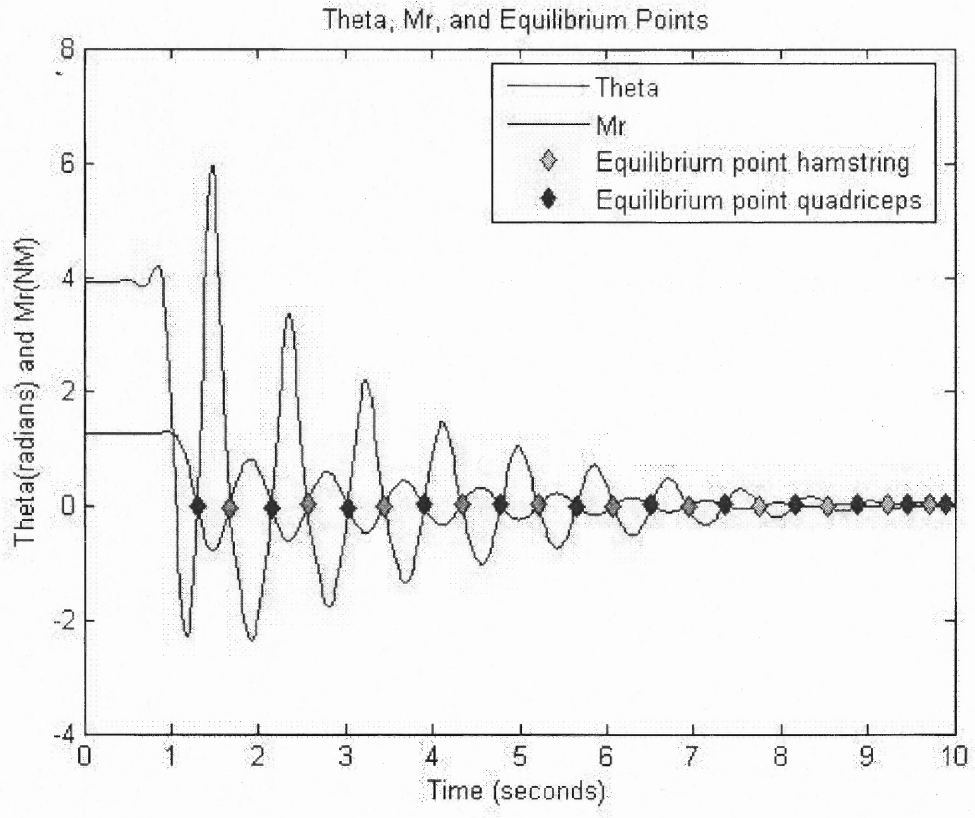

Figure 3.7: θ in black and Mr in blue for the non-spastic subject. When Mr is equal to zero the corresponding θ is the equilibrium point. Equilibrium points for flexion are pictured in red and extension in blue.

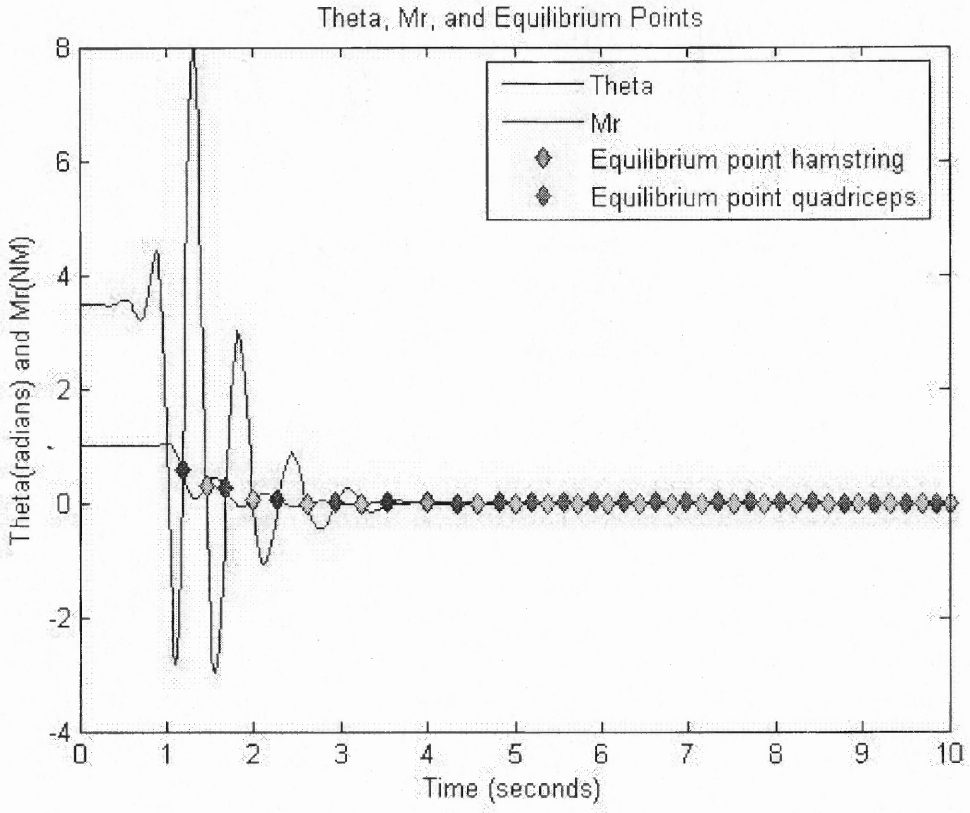

Figure 3.8: θ in black and M*r* in blue for the spastic subject. When Mr is equal to zero the corresponding θ is the equilibrium point. Equilibrium points for flexion are pictured in red and extension in blue. Note that the θ values in early swing are non-zero.

As stated previously, M*r* equal to zero is approximately at the same location where acceleration equal to zero. An illustration of this is pictured below.

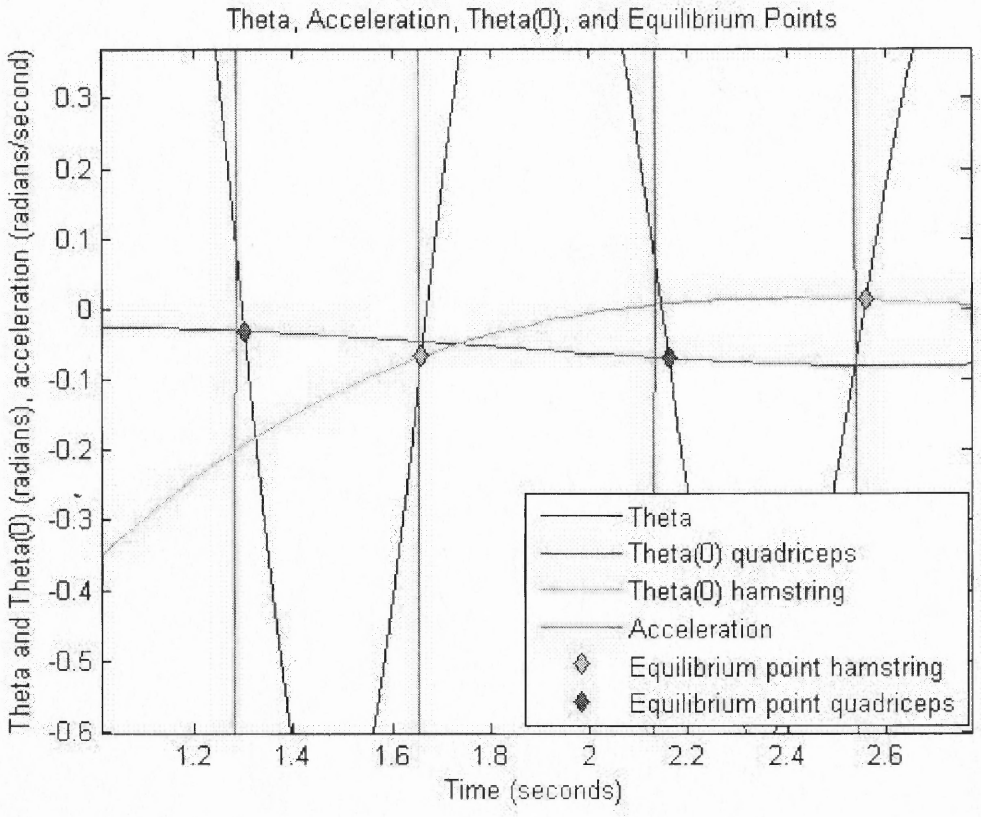

Figure 3.9: Close-up plot showing that where Mr = 0 acceleration is also close to zero.

Two curves of θ_0 are generated via spline interpolation of the equilibrium points to represent θ_0 of the hamstrings and quadriceps.

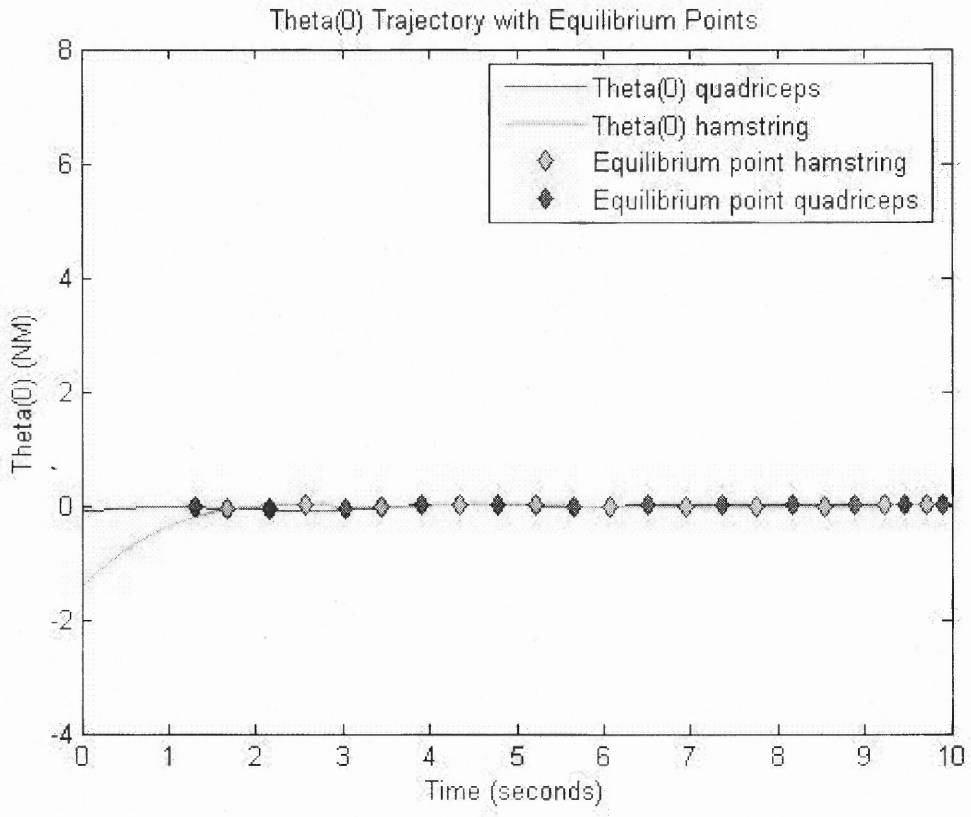

Figure 3.10: Spline interpolation of the equilibrium points to obtain θ_0 for the non-spastic subject.

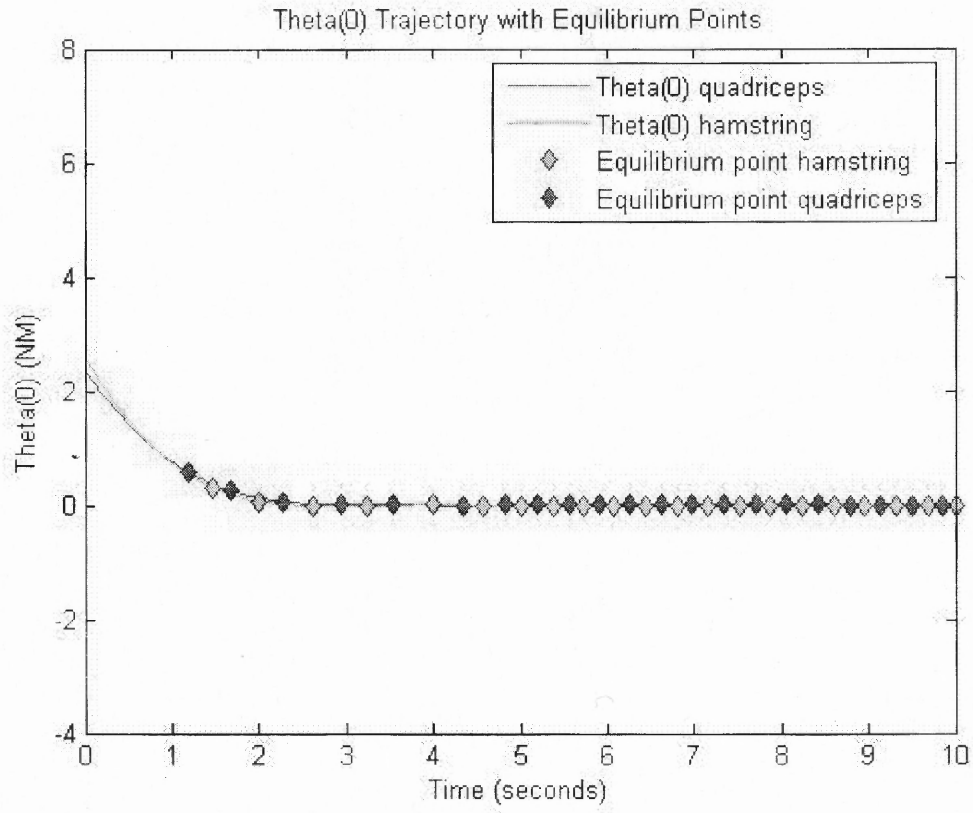

Figure 3.11: Spline interpolation of the equilibrium points to obtain θ_0 for the spastic subject.

K is an estimate of passive elastic stiffness. In a graph of angle versus torque, K is linear and represents the most central area of the graph. By employing a time-varying equilibrium point, we are able to select a constant K. A value for K is obtained by taking the slope of the regression line of the residual torque versus angle plot.

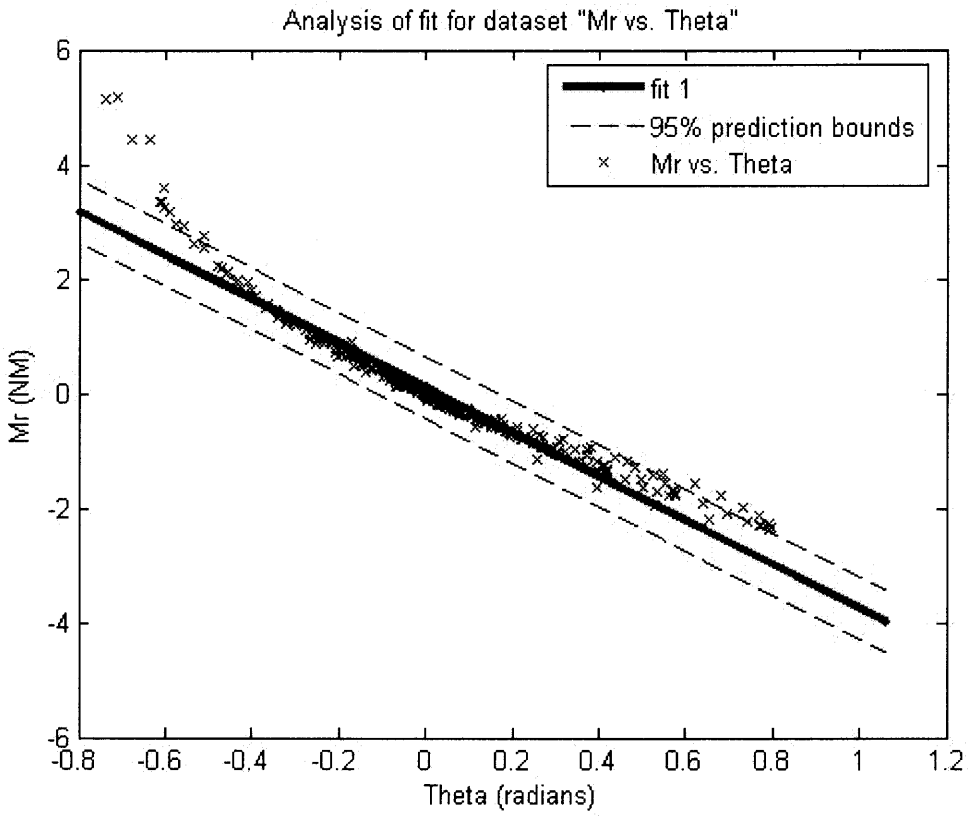

Figure 3.12: Regression line in red for the plot of Mr versus θ. K is the slope of this regression line.

3.3 Experiment Setup

This research has integrated Flock of Birds (Ascension Technology Corporation) sensors with EMG (Grass Telefactor, Astro-Med, Inc.) for data collection. The Flock of Birds and EMG hardware were configured to synchronistically execute through a program written in MATLAB (Math Works, Inc., Natick, MA).

The position of the sensor and electrodes were as follows: To reflect the center of rotation about the knee joint, the Flock of Birds sensor was attached on the sagittal plane, medial-lateral to the knee joint, perpendicular along the knee joint axis of rotation. EMG

electrodes were positioned on the hamstrings and quadriceps. Electrode positioning was verified using an oscilloscope to ensure ideal placement.

Pendulum knee drop data from a female 25-year-old non-spastic subject was collected. The subject was seated on a table with her legs hanging off the side. She sat forward so that the table did not restrict knee rotation, and she was asked to relax so as to not intervene in any way. She was asked to perform the knee-drop test totally relaxed in the three trials. The leg was extended to a comfortable extension as specified by the subject. The test initiated when the leg was released allowing it to fall and oscillate freely.

Figure 3.13: Experimental setup with the Flock of Birds and EMG.

3.4 Instrumentation

3.4.1 Hardware

Flock of Birds is a motion tracking system. A transmitter sends a pulsed DC magnetic field that is tracked by a sensor. The sensor configures the characteristics of the magnetic field into position and orientation. Communication to the host computer is via a serial port. Some of the modifications to the default settings on the Flock of Birds included turning off an internal filter and setting the sample rate to 100 Hz.

Grass Telefactor is the hardware for the EMG collection. AC signals are obtained via electrodes, amplified 5,000 times, and sent through a data acquisition system to the host computer. The sample rate is 1000 Hz.

3.4.2 Software

The MATLAB programs to collect data, process data into the model, and simulate components of the data are discussed below.

The program to model the pendulum knee drop initiates by loading the data. The triplet sensor data was sampled at 50 Hz. The 50 Hz sampling rate for the historical data was lower than ideal, so in the experiment on the female non-spastic subject the sampling rate is increased to 100 Hz. The raw data is filtered with an eighth order, 3 Hz Butterworth filter. Velocity, acceleration, and Mr are calculated from the filtered trajectory. The equilibrium points are obtained by locating the θ where Mr is equal to zero. Since many of the data points are not absolute zero the Mr value represents the

point closest to zero. Then via spline interpolation, θ_0 is obtained for both the hamstring and quadriceps muscles.

EMG was collected for the non-spastic subject. It was collected at 1000 Hz and band-pass filtered between 10 Hz and 499 Hz, pursuant with the Nyquist theorem, using a fourth order Butterworth filter. From the resultant data an envelope was obtained using a 6 Hz, fourth order Butterworth filter. These sample and filter rates were the suggested ranges for myoelectric signals from surface electrodes. [27]

CHAPTER 4

RESULTS AND ANALYSIS

4.1 Triplet Data

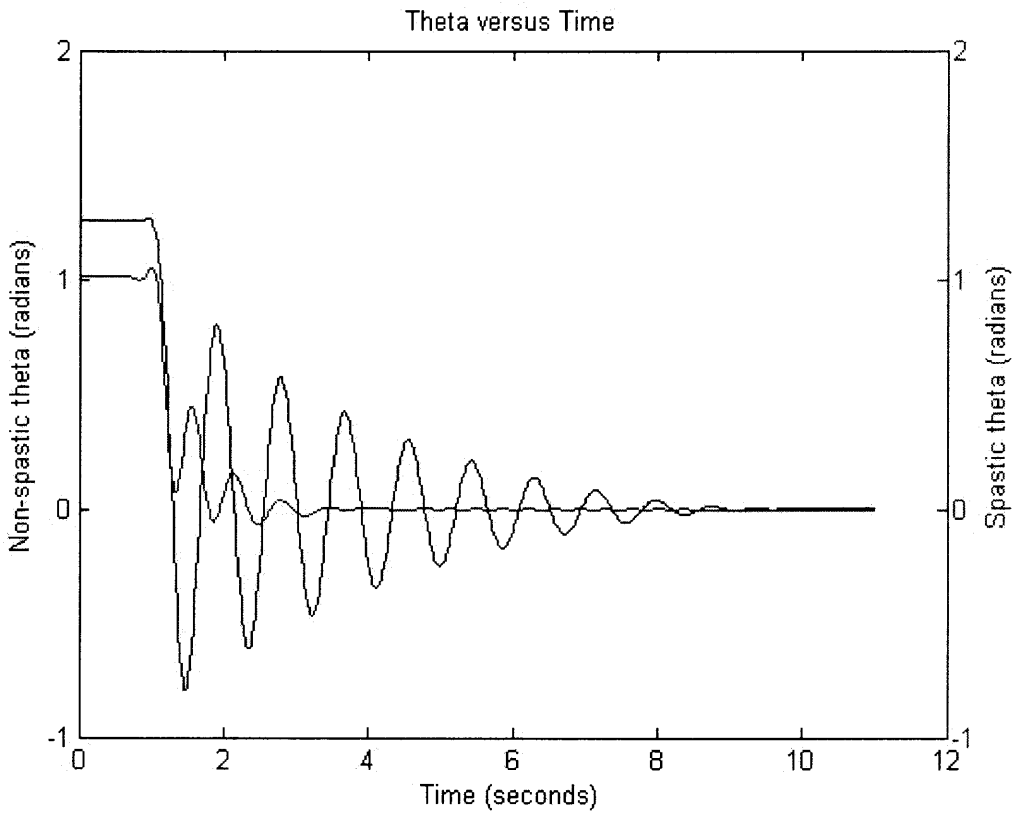

Figure 4.1: Plot of the trajectory of the spastic subject in green and the non-spastic subject in blue.

The spastic trajectory is noted by fewer oscillations, decreased duration of oscillations, decreased amplitude of the first backward swing, and decreased relaxation index—defined as the magnitude of the first backward swing divided by the difference between the starting and resting angles. [13] Note that the data was padded with 50

samples to obtain more accurate calculations of velocity and acceleration. Subsequent plots will show only the trajectory from the point where the leg is released.

The model fit without the addition of M*r* is pictured below for non-spastic and spastic subjects. The spastic and non-spastic damping is found to be 0.125.

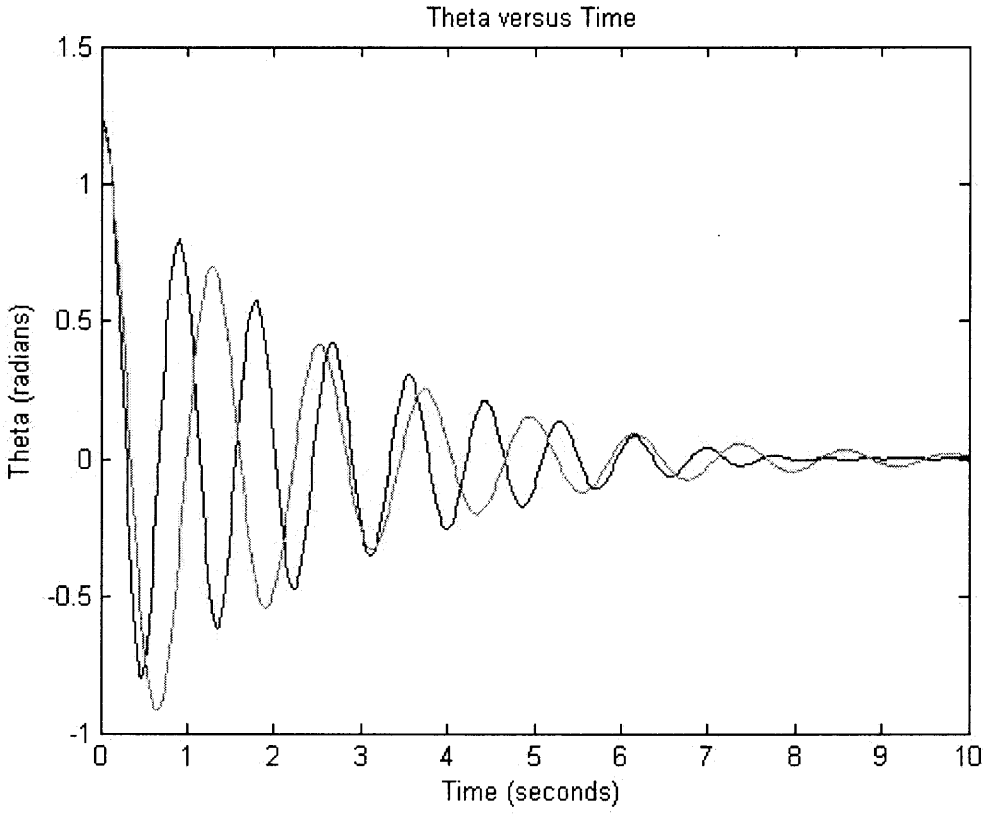

Figure 4.2: Plot of the trajectory versus time. The blue plot is the non-spastic subject and the green plot is the Simulink model fit.

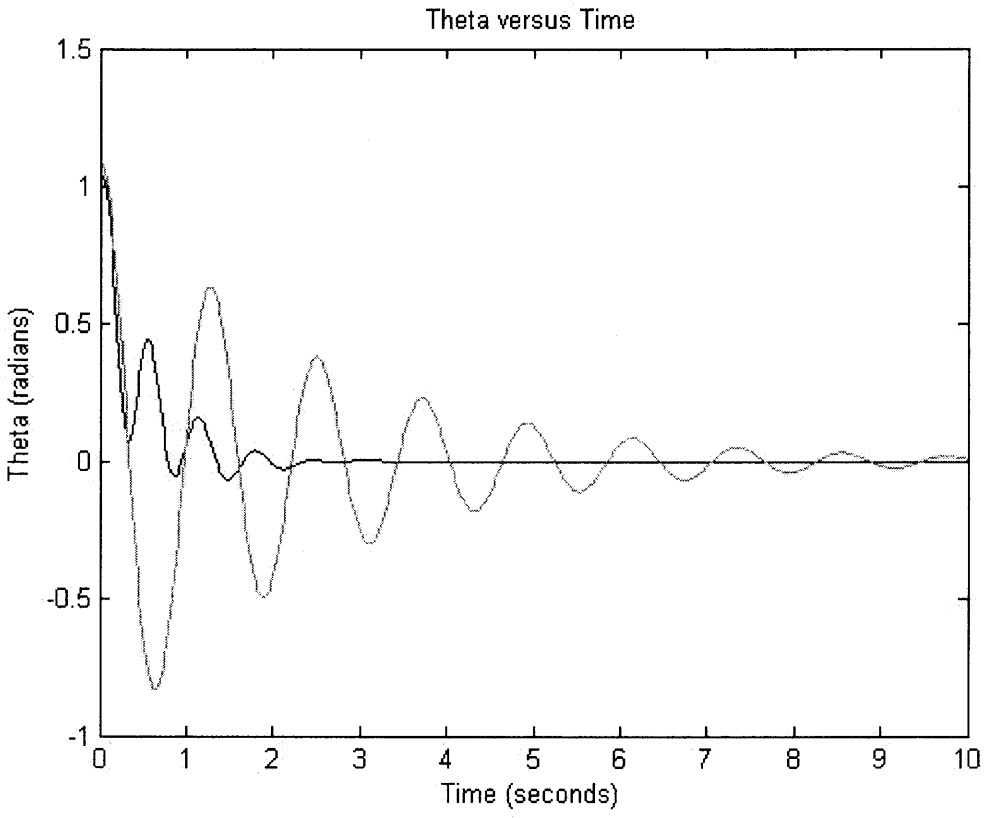

Figure 4.3: Plot of the trajectory versus time. The blue plot is the spastic subject and the green plot is the Simulink model fit.

Residual moment, M*r*, is calculated by taking the difference of the green and blue plots. The following are graphs of M*r* versus time for non-spastic and spastic subjects, respectively.

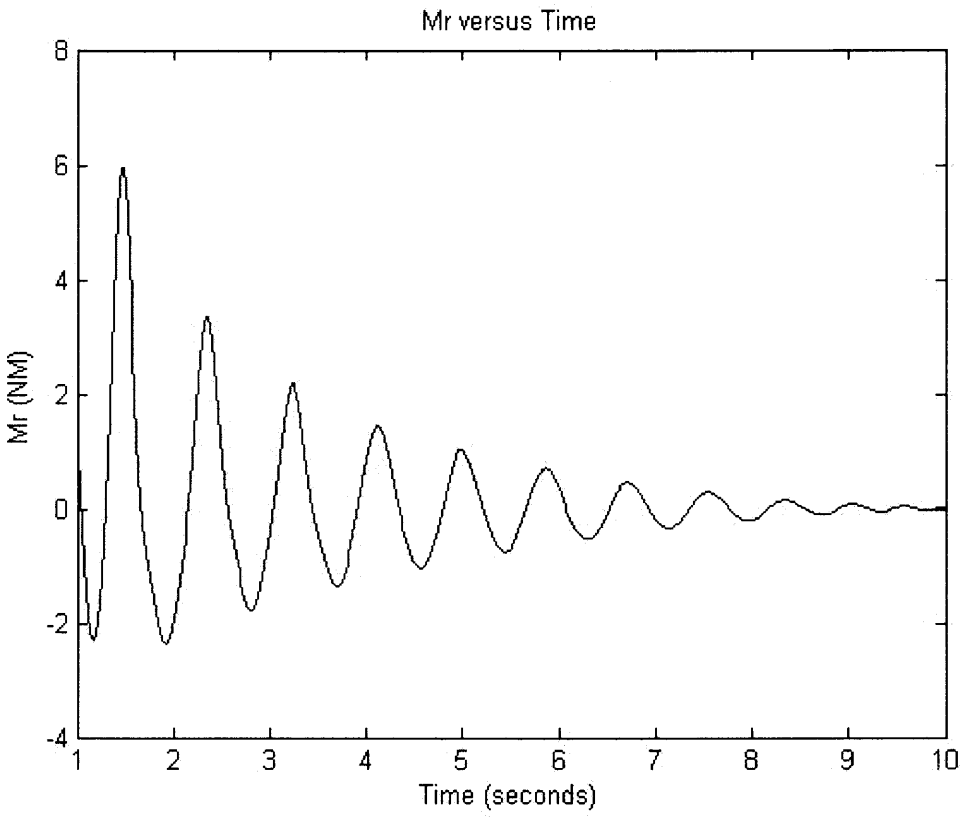

Figure 4.4: Plot of the residual moment, M*r*, versus time for the non-spastic subject.

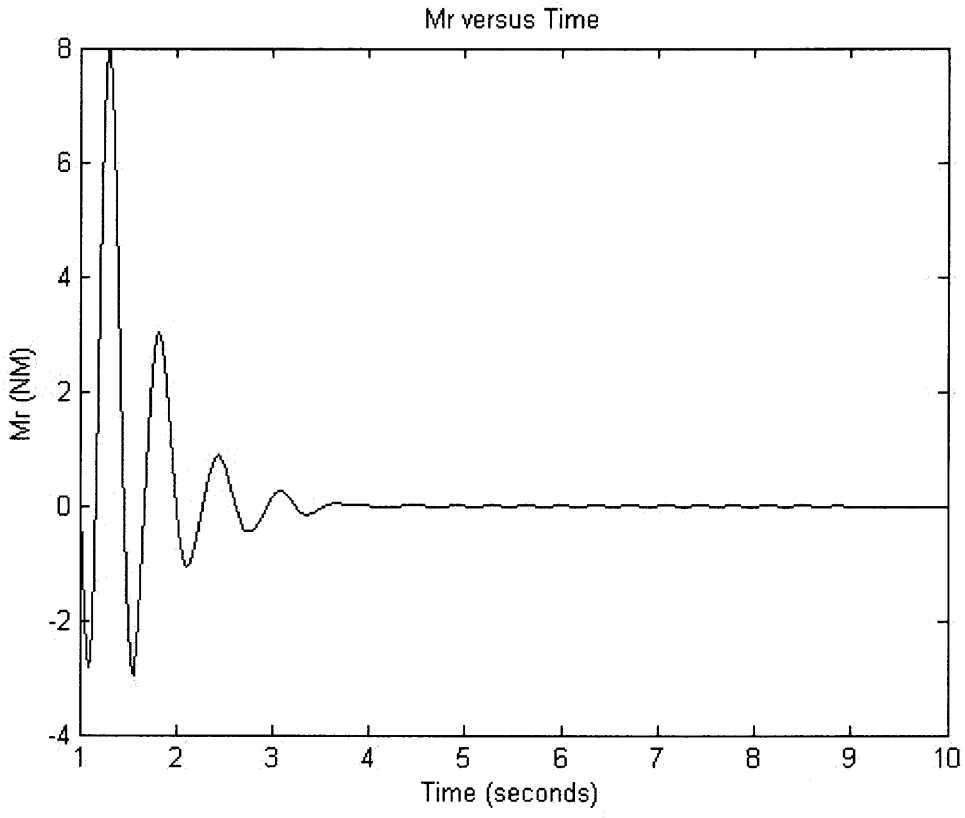

Figure 4.5: Plot of the residual moment, M*r*, versus time for the spastic subject.

Note the onset of torque for the spastic subject occurs sooner than for the non-spastic subject. Also note that the first torque input is larger for the spastic subject.

The following plot shows the residual moment, Mr, versus time for the non-spastic subject. Note the linearity in the central region. The slope of the regression line in this central region represents the passive elastic stiffness, K, and is found to be 3.22 NM in this model.

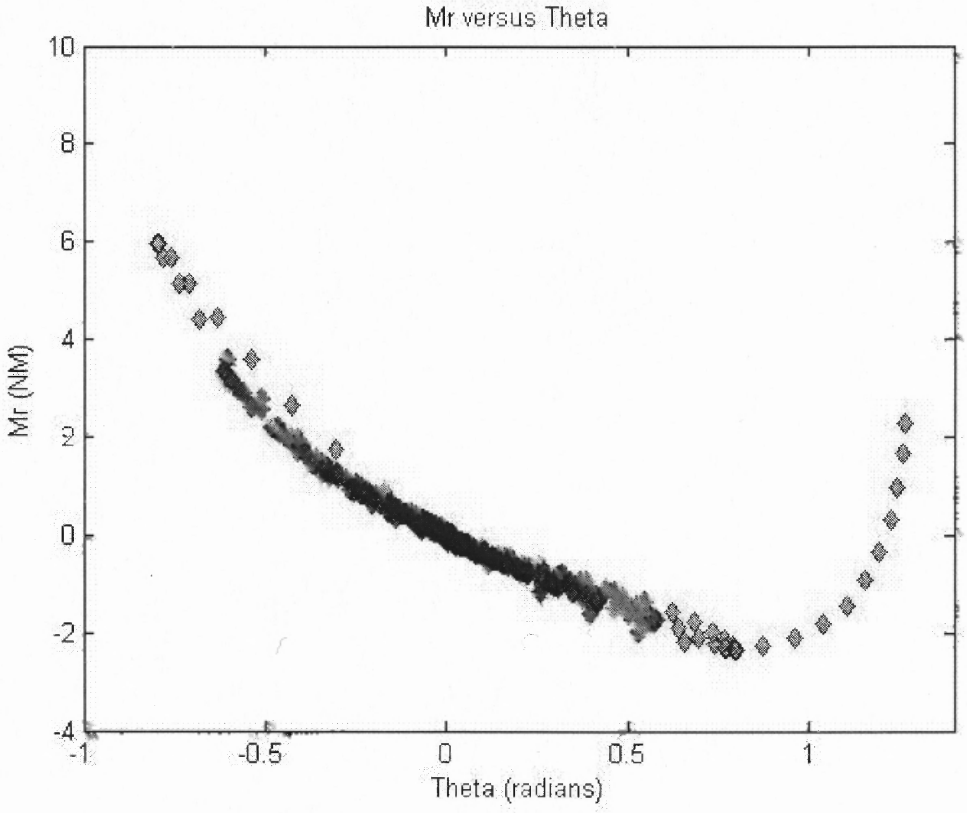

Figure 4.6: Plot of the trajectory, θ, versus residual moment, M*r*, for the non-spastic subject.

The trajectory versus residual torque plot indicates how nonlinear stiffness can be at the outliers. This observation was also noted by Lin and Rymer. McFaull and Lamontagne also noted that at extreme ranges of motion the passive moments play a more dominant role. [17]

By virtue of the way M*r* is calculated, the torque will contain the torque necessary to hold the leg prior to release. A better representation of the initial passive elastic torque prior to release would be available if a holding torque were implemented into the model.

Nordmark and Andersson cite that a handheld force transducer can be used to measure resistance to passive motion. [7] This will be explored in future work.

Figure 4.7 shows the non-linear behavior of the trajectory versus residual torque in the spastic subject. The magnitude of the non-linearity is so large that a value for passive elastic stiffness, K, cannot be isolated from the plot. This plot proves the central problem of isolating passive stiffness from reflex stiffness, as discussed in the background section.

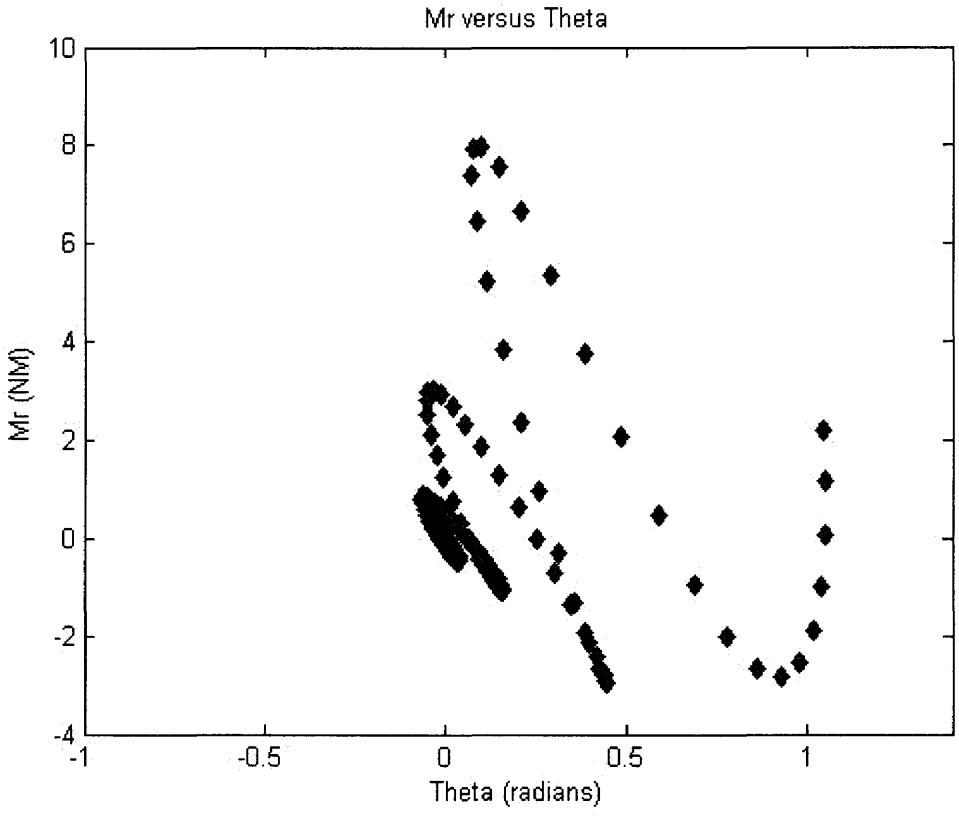

Figure 4.7: Plot of the trajectory, θ, versus residual moment, M*r*, for the spastic subject.

In attempts to linearize this plot to isolate a passive stiffness, this research implements θ_0. To account for the fact that there is not an oscillation about zero in

spastic trajectories, the K term is adjusted from Kθ to K (θ - θ_0) where θ_0 is a time-varying curve based on equilibrium point changes. [15]

Figure 4.8 shows the spastic trajectory, θ, in black, spastic θ_0 and equilibrium points for the quadriceps in red and hamstring in green.

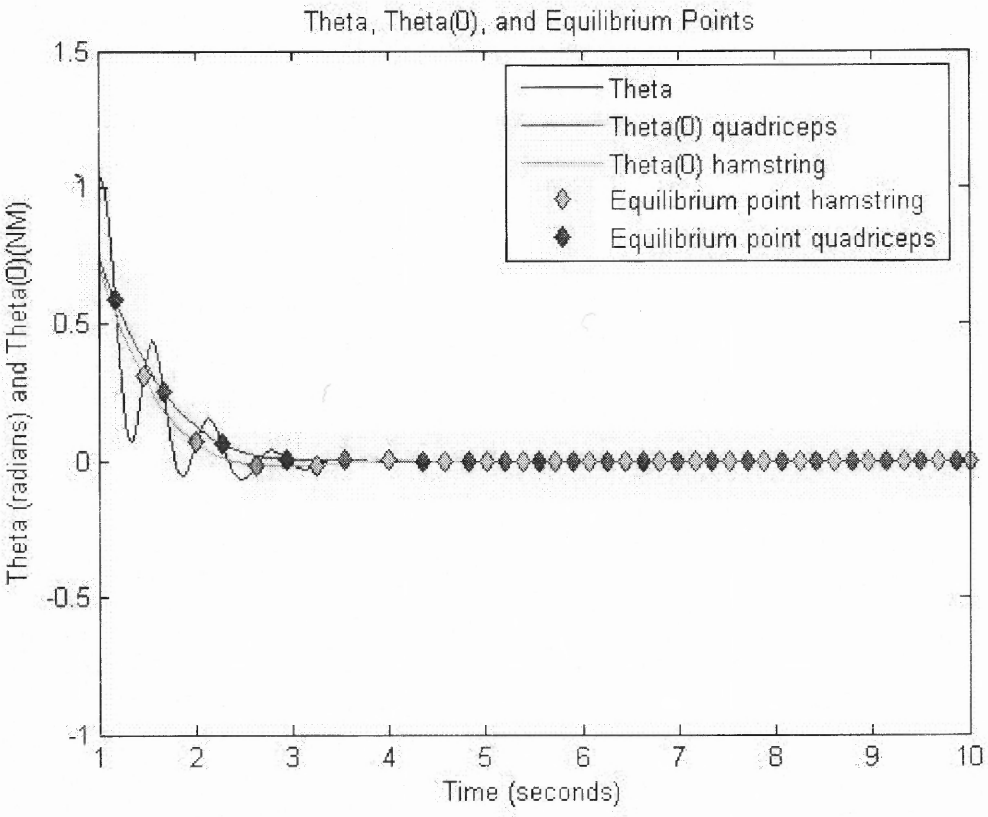

Figure 4.8: Plot of the spastic trajectory, θ, in black and spastic θ_0 and equilibrium points for the quadriceps (red) and hamstrings (green).

Both θ_0 curves exhibit a decaying exponential trajectory. The dynamic character of θ_0 is equated with the hyperactivity of the stretch reflex.

Inputting θ_0 into the stiffness moment gives a basically linear plot of trajectory versus residual torque.

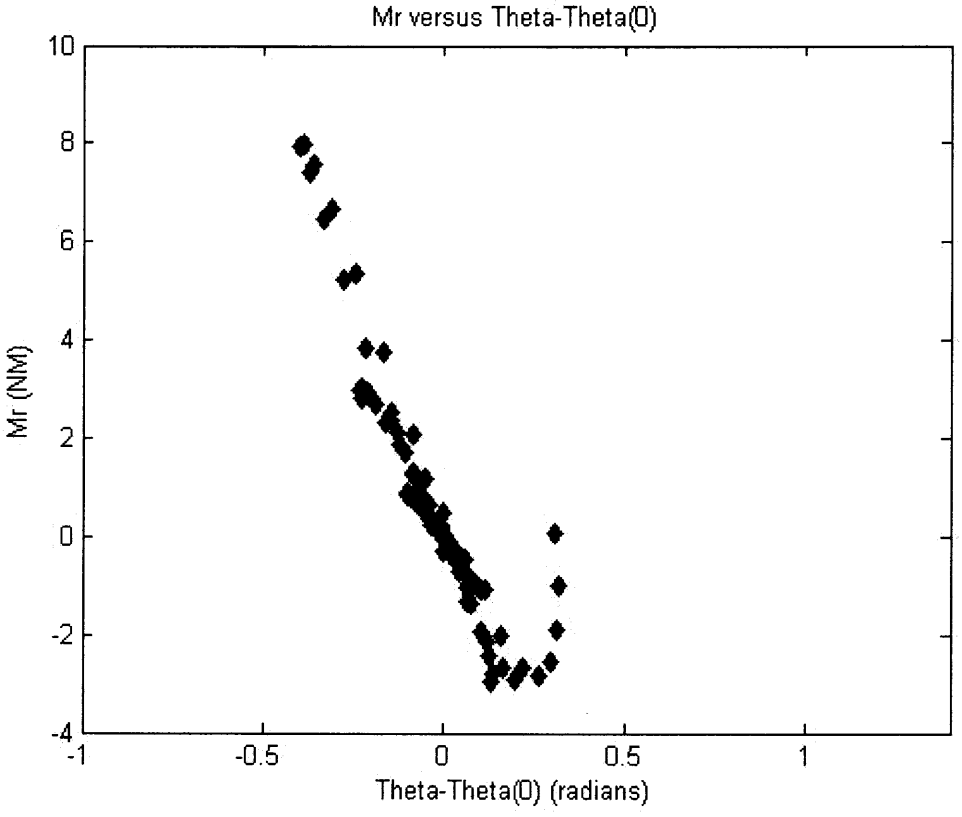

Figure 4.9: Plot of the trajectory, $\theta - \theta_0$, versus residual moment, M*r*, for the spastic subject.

Note that the plot is essentially linear. This allows for the calculation of passive joint stiffness—16.09 NM. Since there appears to be a several linear intervals, the piecewise range of K lies within 10.1 to 17.9 NM. Regardless of whether K is considered as constant or piecewise, it is higher than that of his sibling without cerebral palsy (3.22 NM). K is equated with the clinical concept of tone. This is in line with the clinical definition of spasticity as a hyperactivity of the stretch reflex and increase in tone.

Graphs of the non-spastic θ_0 show curves that are close to linear about zero. In the first three swings however there appears to be a slight disparity from zero.

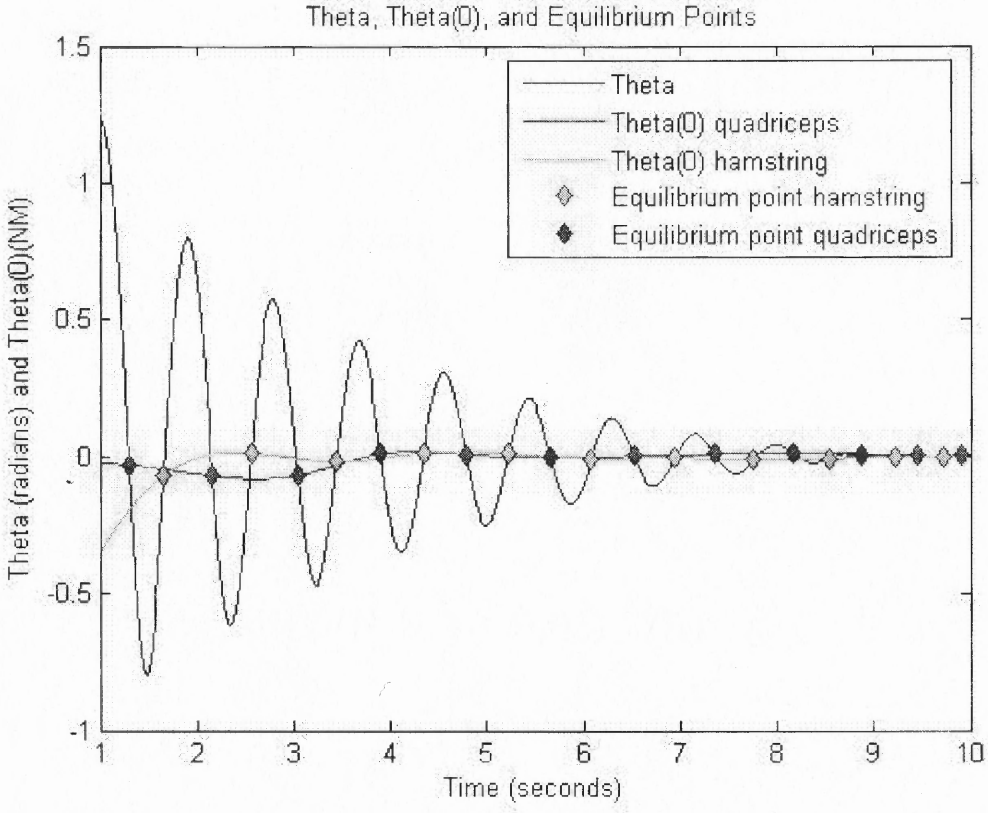

Figure 4.10: Plot of the non-spastic trajectory, θ, in black and spastic θ_0 and equilibrium points for the quadriceps (red) and hamstrings (green).

The existence of nonlinearity at extreme range of motion is a hypothesis held by many scientific papers that goes unproven. The experiment on a non-spastic subject will attempt to demonstrate a basis for this nonlinear torque.

4.1.1 Model Accuracy

The following is an evaluation of the model's accuracy. Parameters are changed to show which is the most important to the overall system. Parameters are also validated with existing values from scientific papers.

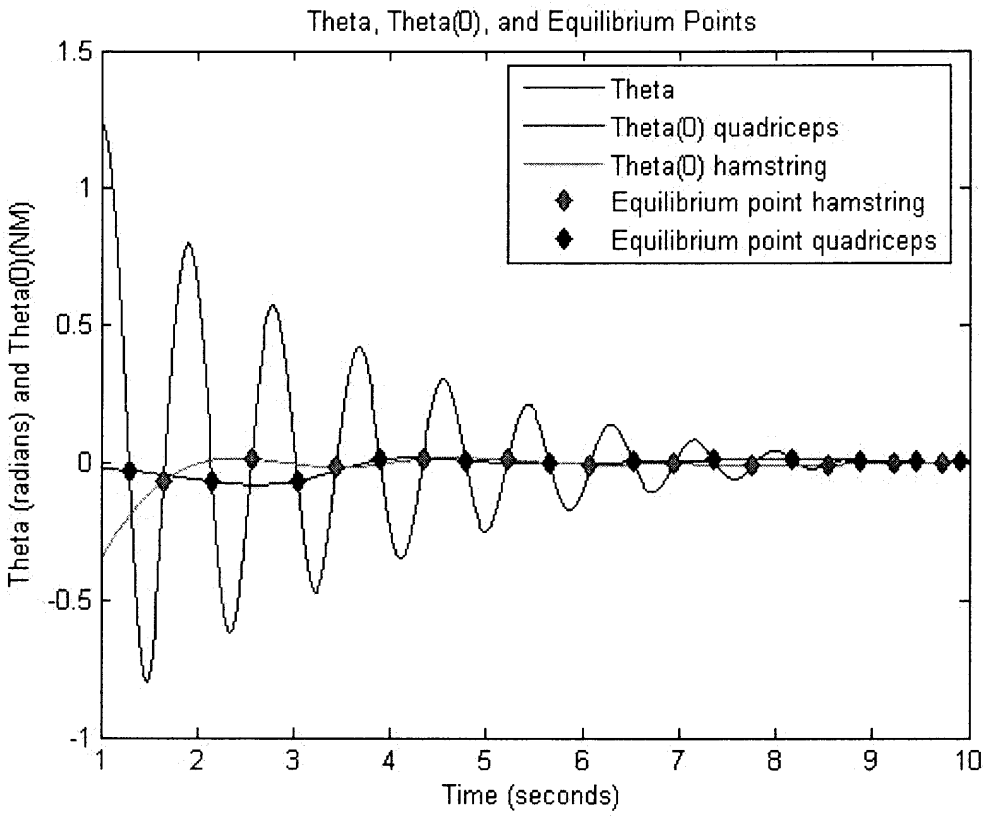

Figure 4.10: Plot of the non-spastic trajectory, θ, in black and spastic θ_0 and equilibrium points for the quadriceps (red) and hamstrings (green).

The existence of nonlinearity at extreme range of motion is a hypothesis held by many scientific papers that goes unproven. The experiment on a non-spastic subject will attempt to demonstrate a basis for this nonlinear torque.

4.1.1 Model Accuracy

The following is an evaluation of the model's accuracy. Parameters are changed to show which is the most important to the overall system. Parameters are also validated with existing values from scientific papers.

Upon reaching a good fit for the damping coefficient (0.125) through trial and error, the model was validated with the values from the Fee and Foulds study. The damping coefficient was within 2.8% of Fee and Foulds's value of B (0.1215 ± 0.0005). Similarly, our calculated spring coefficient of 3.22 was in a similar range to the 3.68 ± 0.01 obtained in the Fee and Foulds experiment.

Adjusting model parameters allows for identification of what factors M*r* is dependent on. Many have debated whether spastic torque is velocity and/or position dependent. By altering the values of position, velocity, and acceleration it should be apparent which factor M*r* is most dependent on. The following adjustments are made using the non-spastic triplet trajectory.

The definition of spasticity is "velocity-dependent" increase in stretch reflexes. Since this model isolates all residual torque, the plot should significantly change when the M*d* component is increased. Below is a plot of M*r* versus Theta when the damping times velocity is doubled. Doubling M*d* serves to delinearize the plot.

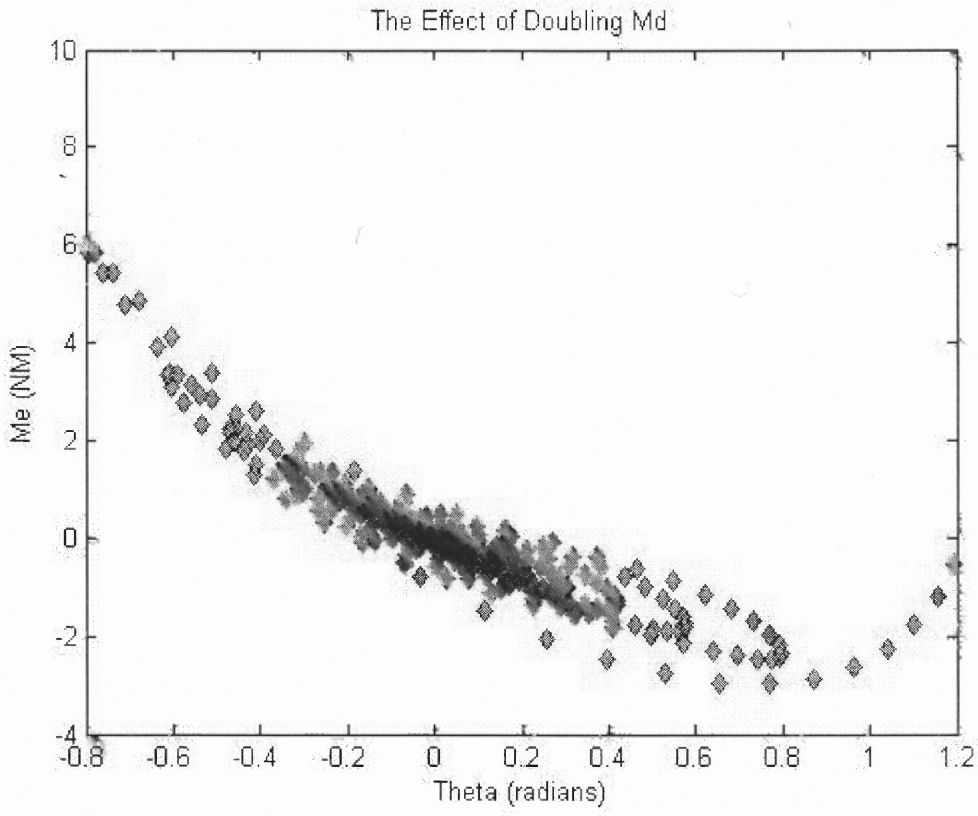

Figure 4.11: Doubling the M*d* serves to delinearize the curve.

When the moment of inertia multiplied by angular acceleration is doubled the result is increased passive elastic stiffness exhibited by the slope of the M*r* versus angle relationship.

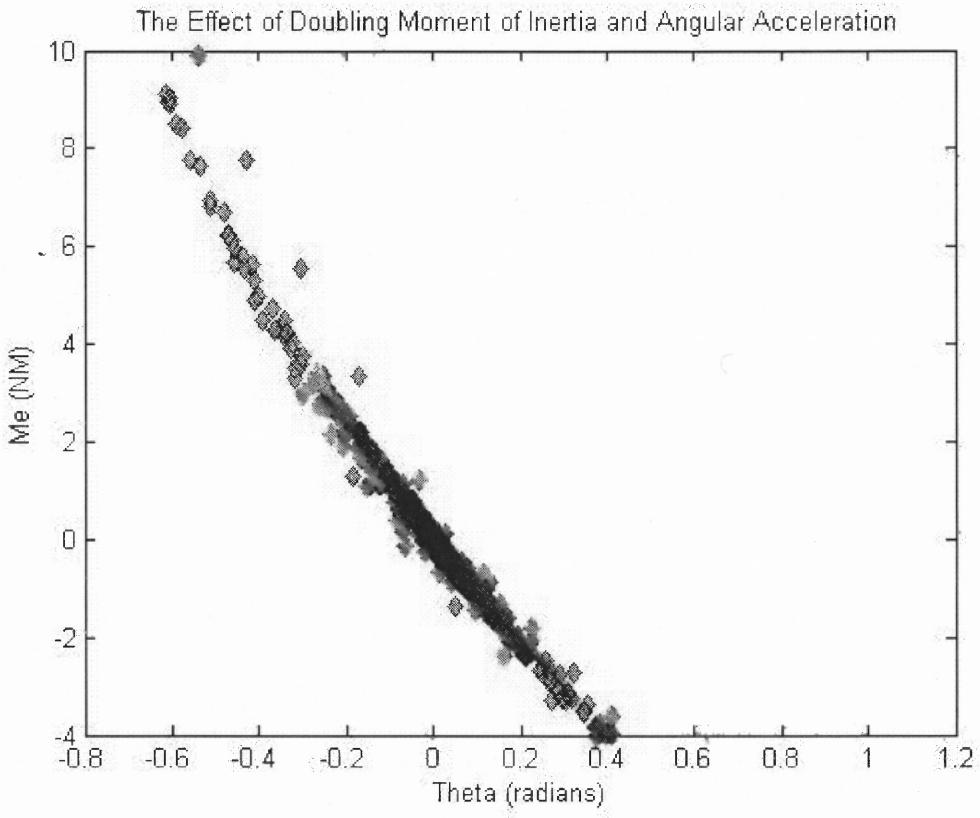

Figure 4.12: Doubling the Iα serves to increase the slope representing passive elastic stiffness, K.

When Mg is doubled, the result is a decrease in passive elastic stiffness as exhibited by the slope of the M*r* versus angle relationship.

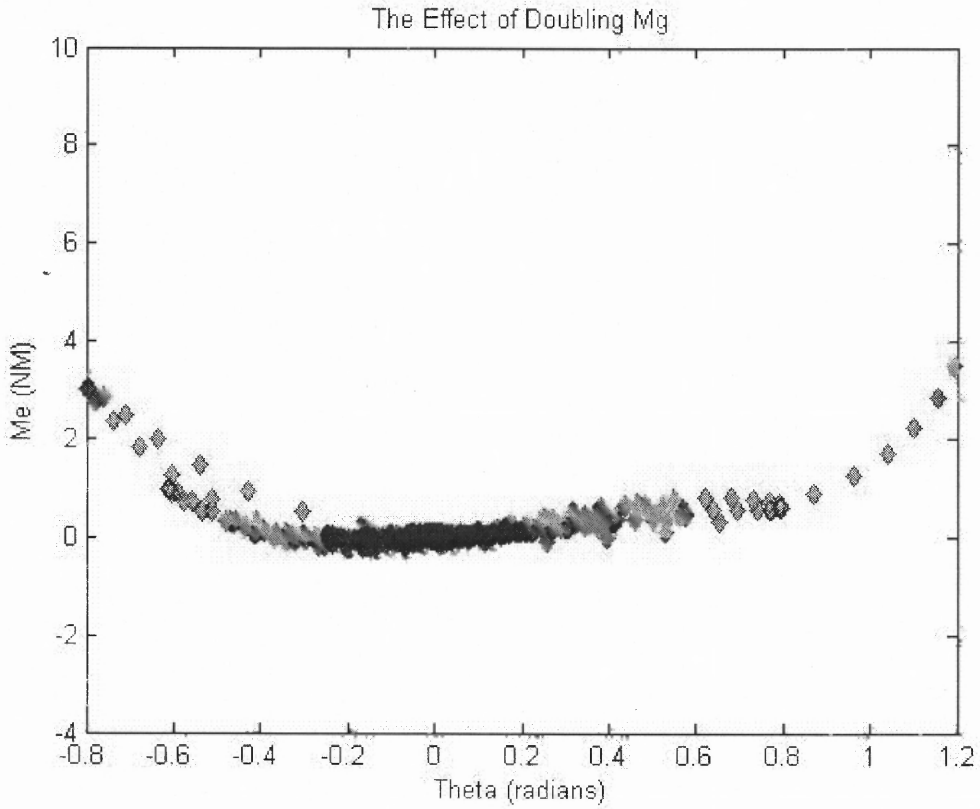

Figure 4.13: Doubling the M*g* serves to decrease the slope representing passive elastic stiffness, K.

From the adjustment of the parameters (position, velocity, or acceleration) it appears that changes are reflected in passive elastic stiffness. As the graphs indicate, doubling Iα and Mg change passive elastic stiffness in the positive and negative direction. The model validated by this finding, since K is not an estimate but a caclulation after all other variables have been obtained. The delinearization, represented by doubling M*d*, indicates that errors in damping will play a large role in the θ_0 calculation. Because of this finding we explore new methods of M*d* calculation in future work

4.2 Non-spastic Control Data

The non-spastic control experiment attempts to quantify nonlinearity at the extreme range of motion as observed in the non-spastic triplet plot.

The following plot is the trajectory, θ, for the non-spastic control subject. Note that there is noise evoked by holding the leg in the air. Since noise due to holding the leg in the air is not an evaluative measure, subsequent plots will show only the trajectory from the point where the leg is released.

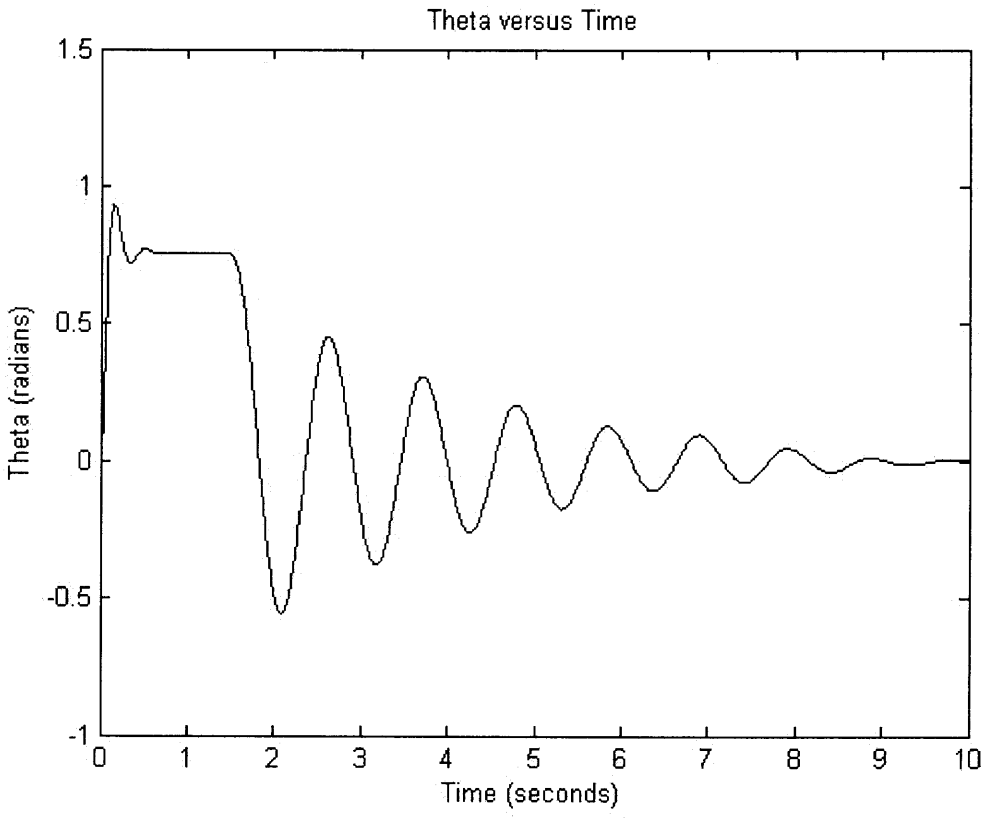

Figure 4.14: Trajectory, θ, of the knee in the pendulum knee drop test for the non-spastic control subject. Note noise due to holding the leg in the air prior to release.

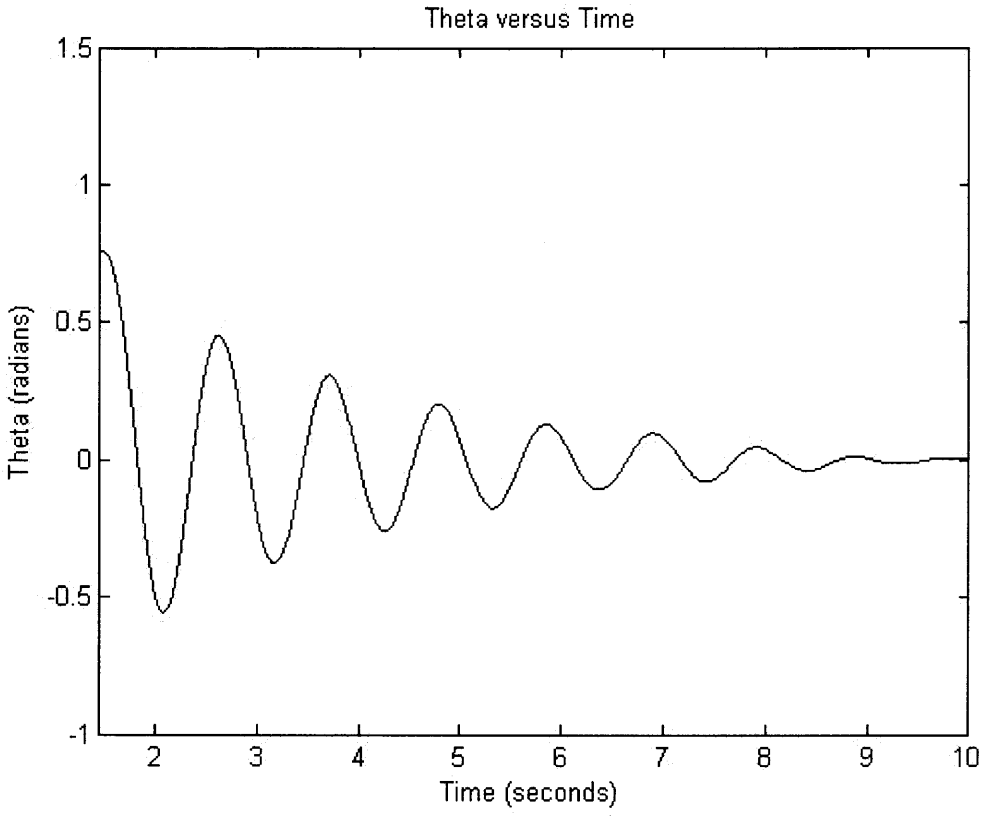

Figure 4.15: Trajectory, θ, of the knee in the pendulum knee drop test for the non-spastic control subject. Subsequent plots will show only the trajectory from the point where the leg is released.

A definition from Fowler *et al.* proves the data viable. They suggest that for healthy subjects a phase plane of angular velocity versus angle should show a "uniform whirlpool" effect and that voluntary activation is shown by changes in the uniform pattern. [13] A phase plane plot of the data collected on the non-spastic subject is noted by irregularities in the phase plans. By this classification it could be suggested that there is muscle activation.

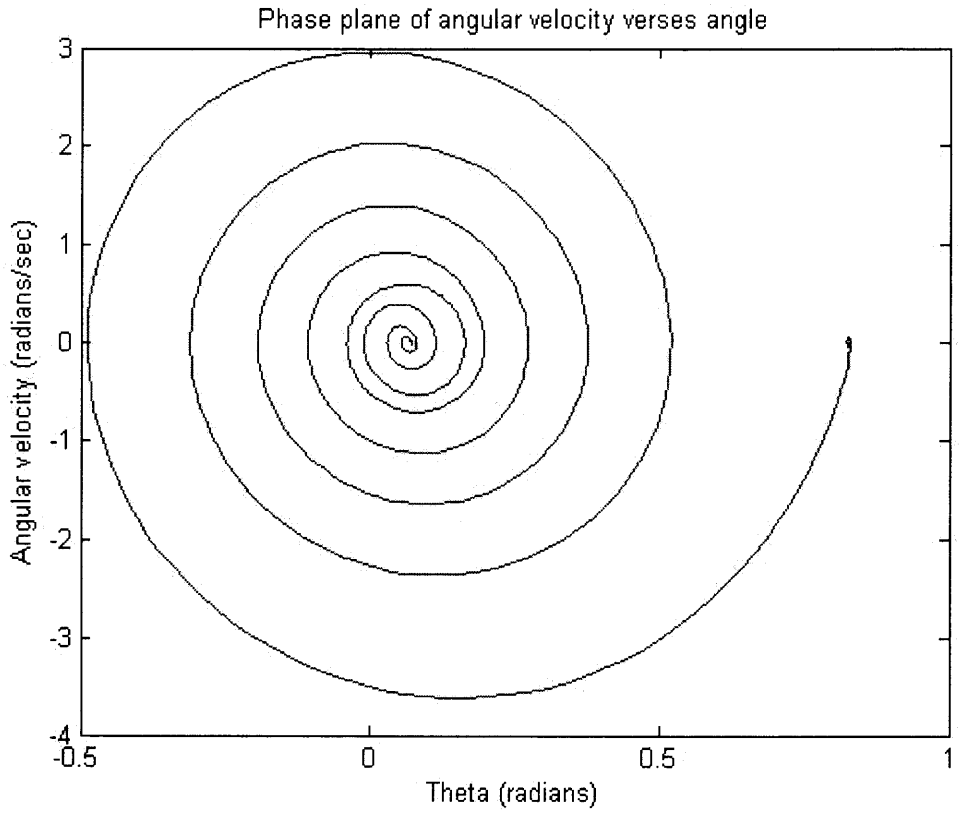

Figure 4.16: A phase plot of angular velocity and trajectory.

Obtaining a damping coefficient was found by trial and error using a Simulink program. The model fit without the addition of M*r* is pictured below for non-spastic control subject. The non-spastic damping is found to be 0.30.

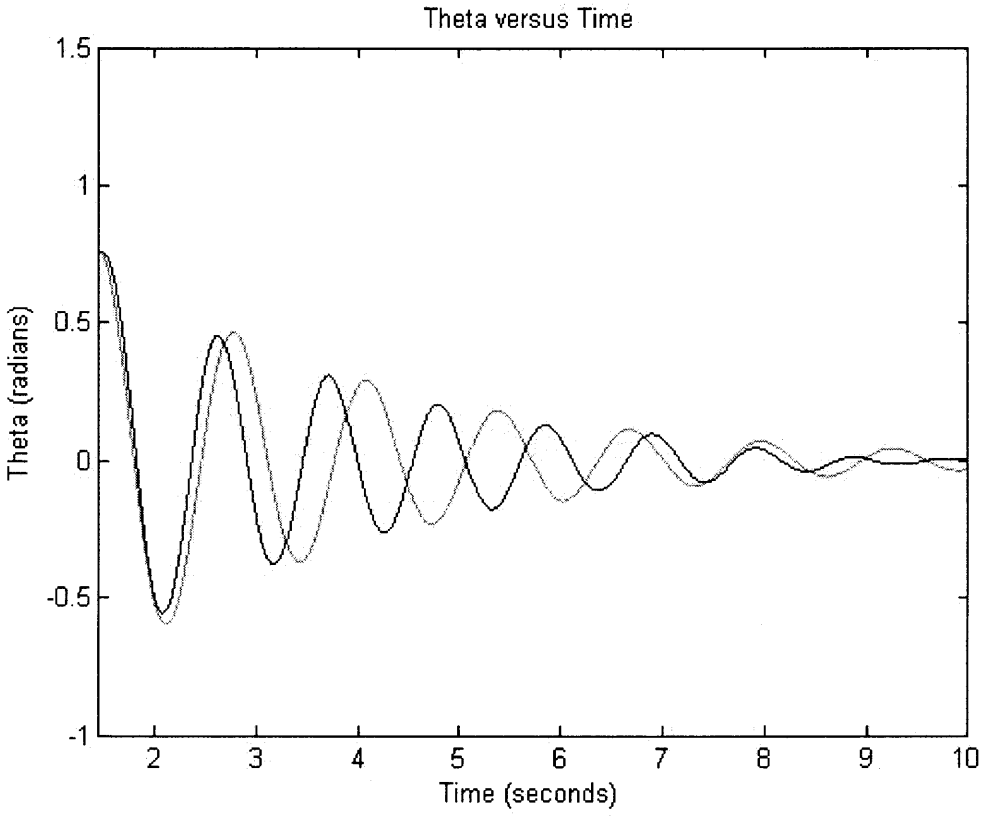

Figure 4.17: Plot of the trajectory versus time. The blue plot is the non-spastic subject and the green plot is the Simulink model fit.

With the parameters M*g*, M*d*, and Iα obtained, M*r* can be calculated on a point-by-point basis. The following plot shows M*r* residual torque versus time for the non-spastic subject.

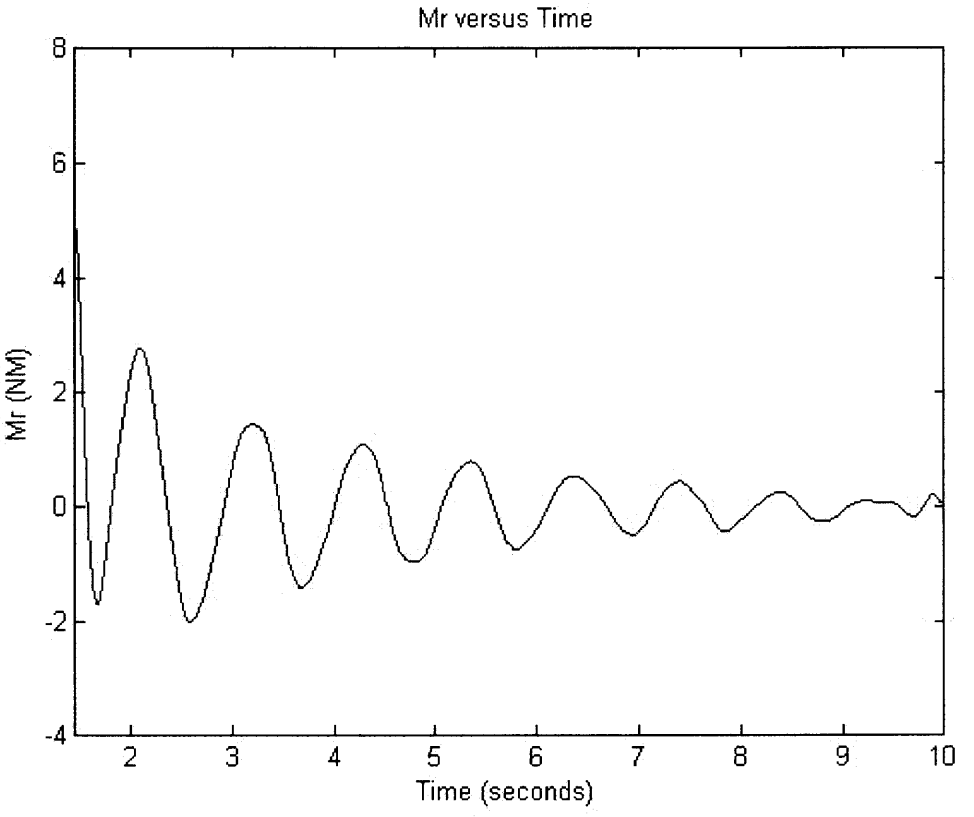

Figure 4.18: Plot of the residual moment, M*r*, versus time.

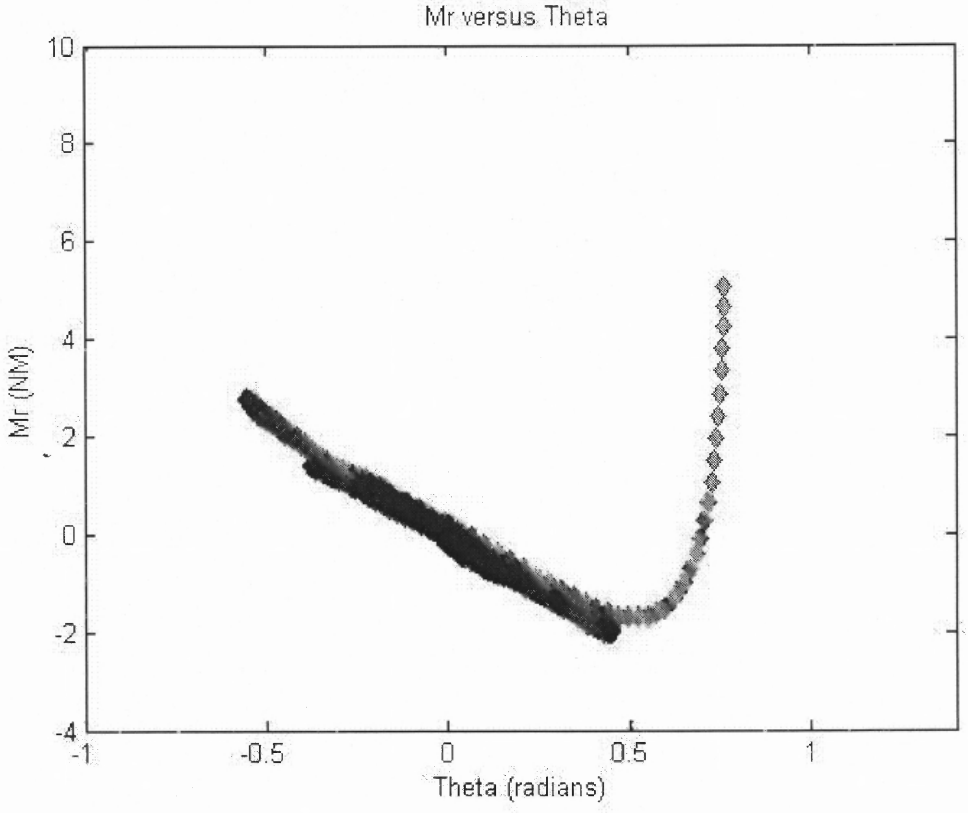

Figure 4.19: Plot of the residual moment, M*r*, versus trajectory, θ.

Figure 4.17 is a plot of the trajectory, θ, versus residual moment, M*r*, for the non-spastic subject. Note the linearity in the central region.

Regression line gives an estimate of elastic stiffness, K, as being 4.478 NM for M_r versus θ. K for M_r versus θ - θ_0 is 4.451. The square of the multiple correlation coefficients, R2, is 0.9794, a small improvement to the graph without θ_0 which was 0.9792. The sum of squared error is 11.25 a nominal improvement to the curve without θ_0 which was 11.30.

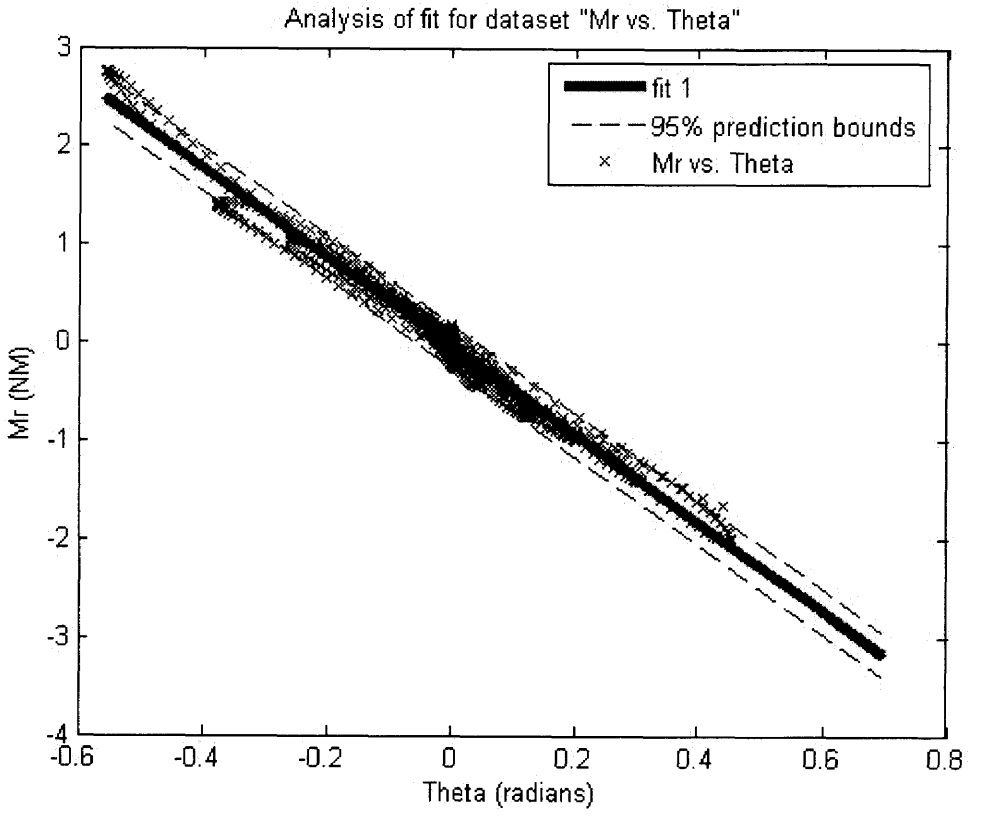

Figure 4.20: Plot of the M_r versus θ relationship in purple, regression line in red, and 95% confidence bounds in blue.

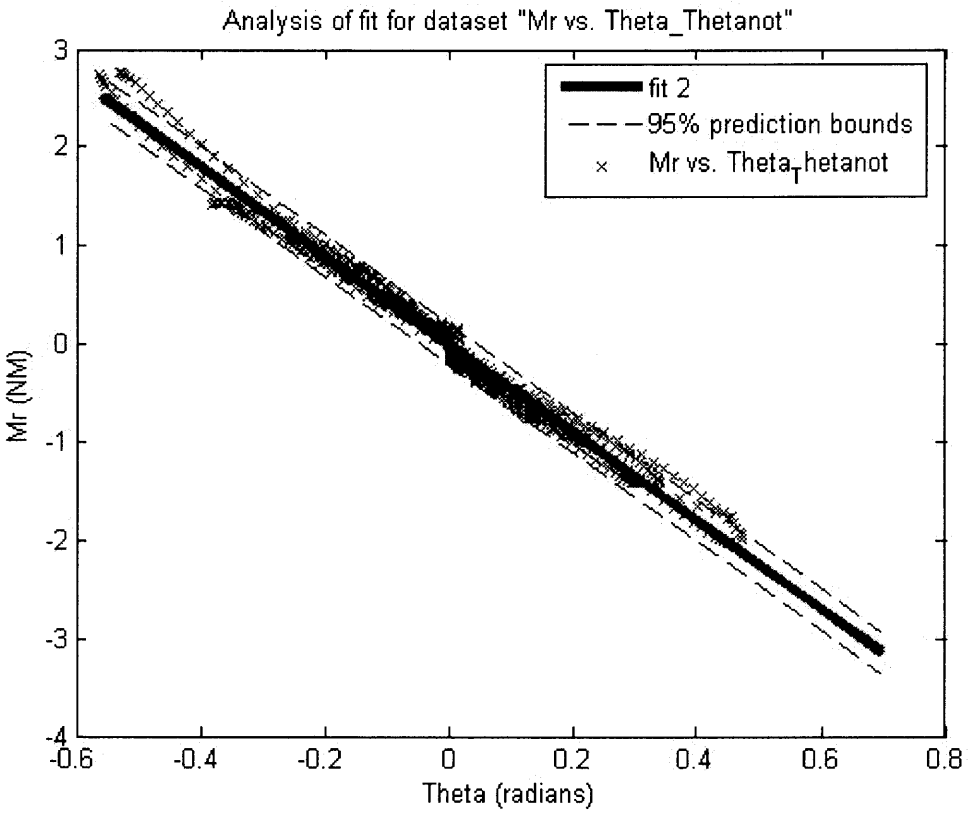

Figure 4.21: Plot of the M*r* versus $\theta - \theta_0$ relationship in purple, regression line in red, and 95% confidence bounds in blue.

The graph of M*r* versus θ appears linear. Upon closer look, the first three swings lie outside of M*r* equal to zero indicating nonlinearity, although nominal.

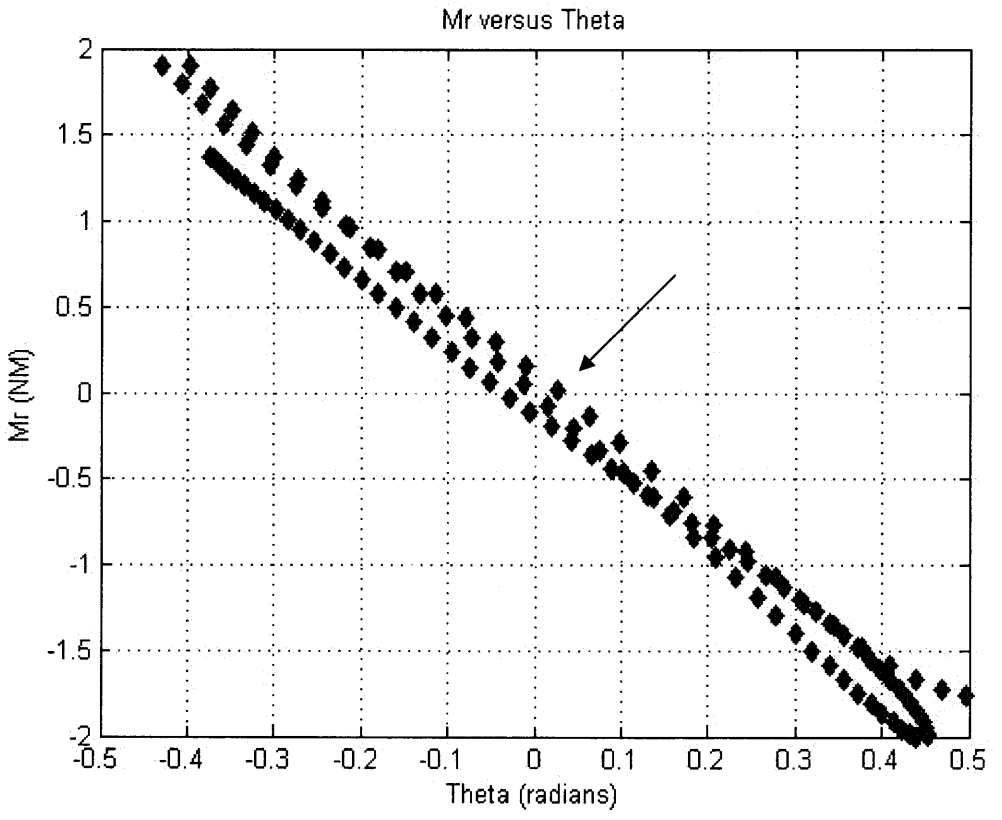

Figure 4:22: Close-up plot of M*r* versus θ showing the deviation from zero.

The following plot shows how the model can make improvement to even the smallest nonlinearity. In the first three swings, which typically represent nonlinearity even in non-spastic subjects, note how the trajectory migrates closer to zero.

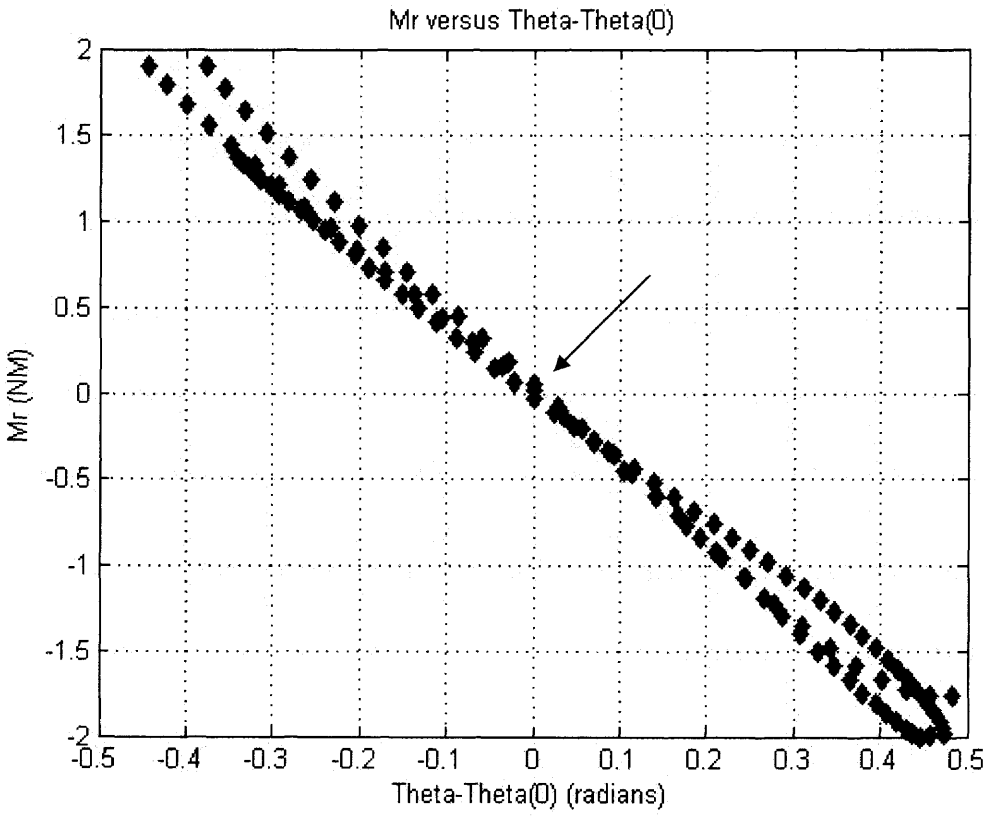

Figure 4.23: Close-up plot of M*r* versus θ showing the migration to zero by the addition of θ_0.

The improved graph of Mr versus $\theta - \theta_0$ is plotted below. While the change is visibly unnoticeable, the statistical analysis shows improvement.

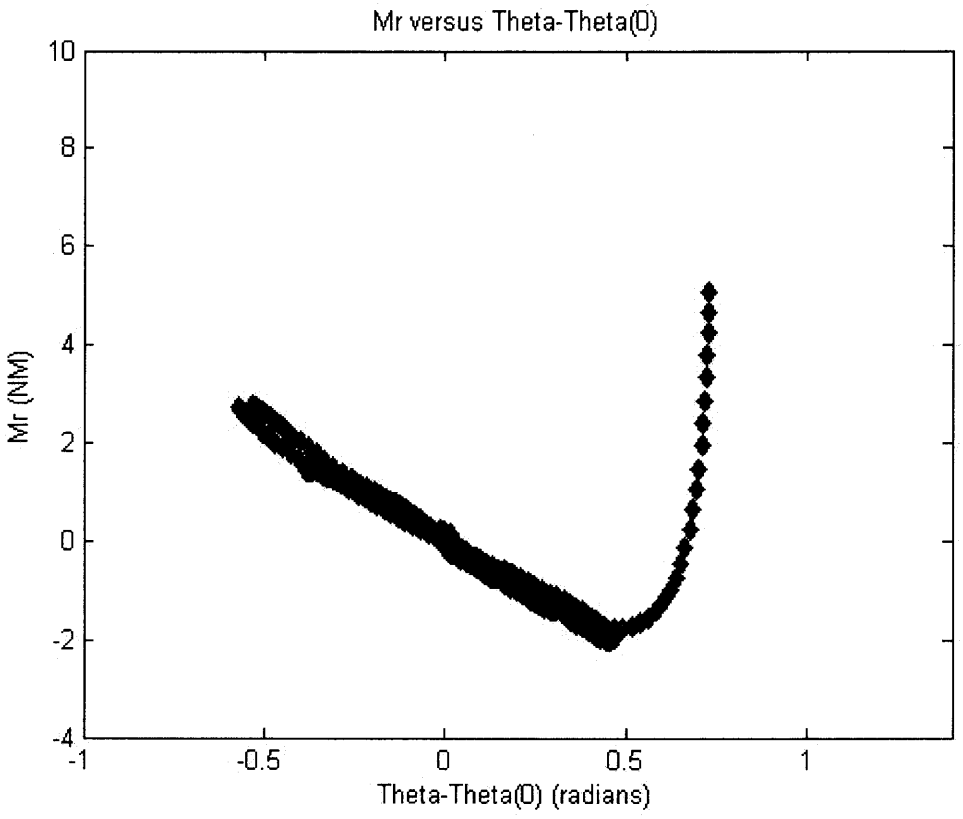

Figure 4.24: Plot of the residual moment, M*r*, versus trajectory, $\theta - \theta_0$.

θ_0 essentially moves the plot of M*r* versus θ closer to zero. This indicates that there must a change in equilibrium point in the non-spastic subject. The following plot illustrates the change in equilibrium points for the quadriceps and hamstring muscles. Note that the changes in equilibrium points occur in early swing, as hypothesized.

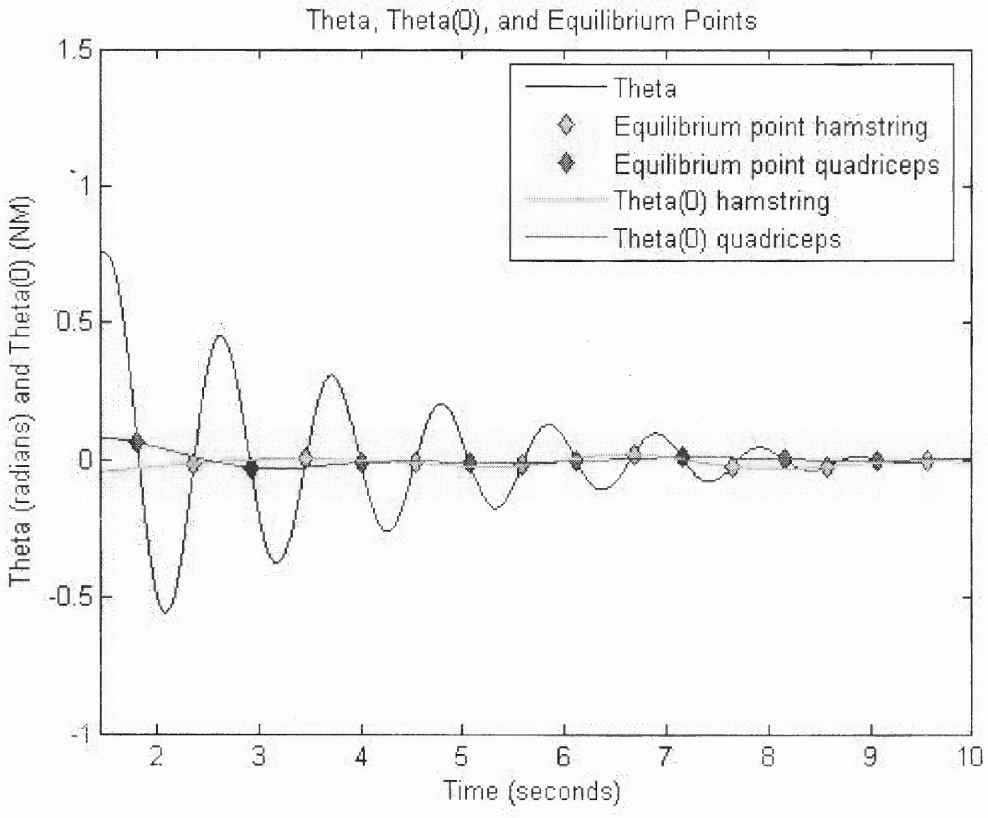

Figure 4.25: Equilibrium points for the hamstring (green) and quadriceps (red), θ_0 trajectories for the hamstring (green) and quadriceps (red), and θ in black.

EMG will further prove the existence of nonlinearity, since the use of EMG in conjunction with the pendulum knee drop test shows muscle activation. If EMG activity in the quadriceps is exhibited in the early swing it could be hypothesized that there is muscle activation in early swing and high velocity. In the following plot note the EMG activity and equilibrium point.

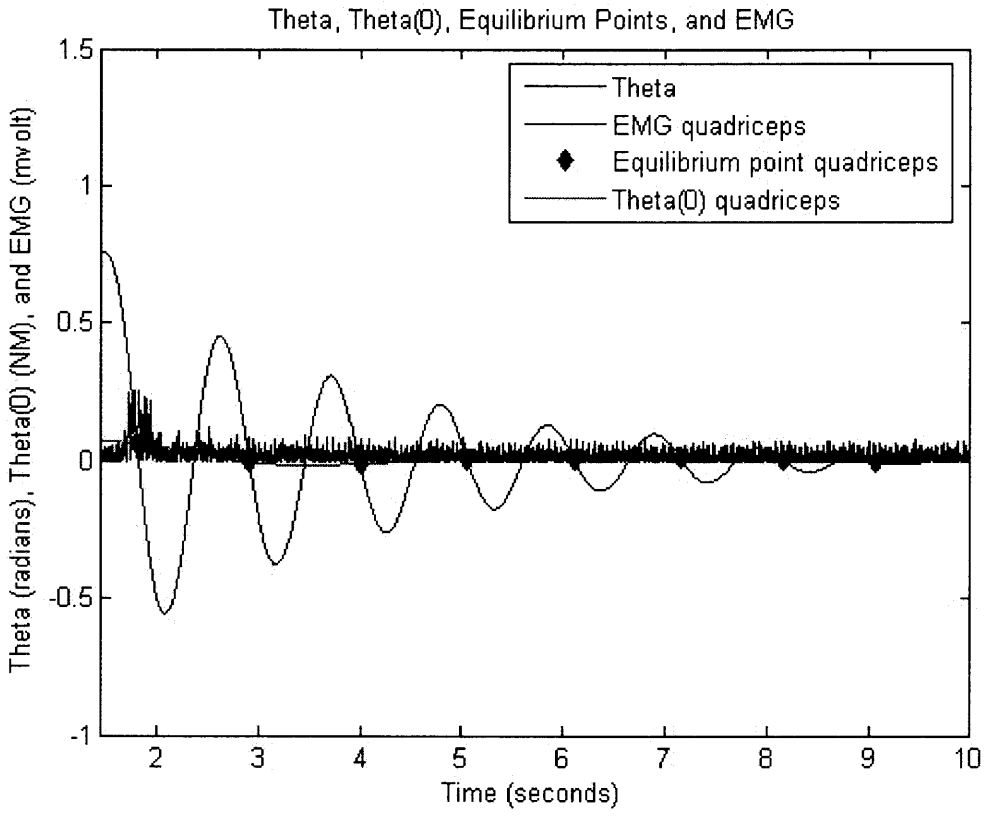

Figure 4.26: A plot of trajectory, θ, in black, EMG of the quadriceps in blue, and equilibrium points and θ_0 trajectory in red.

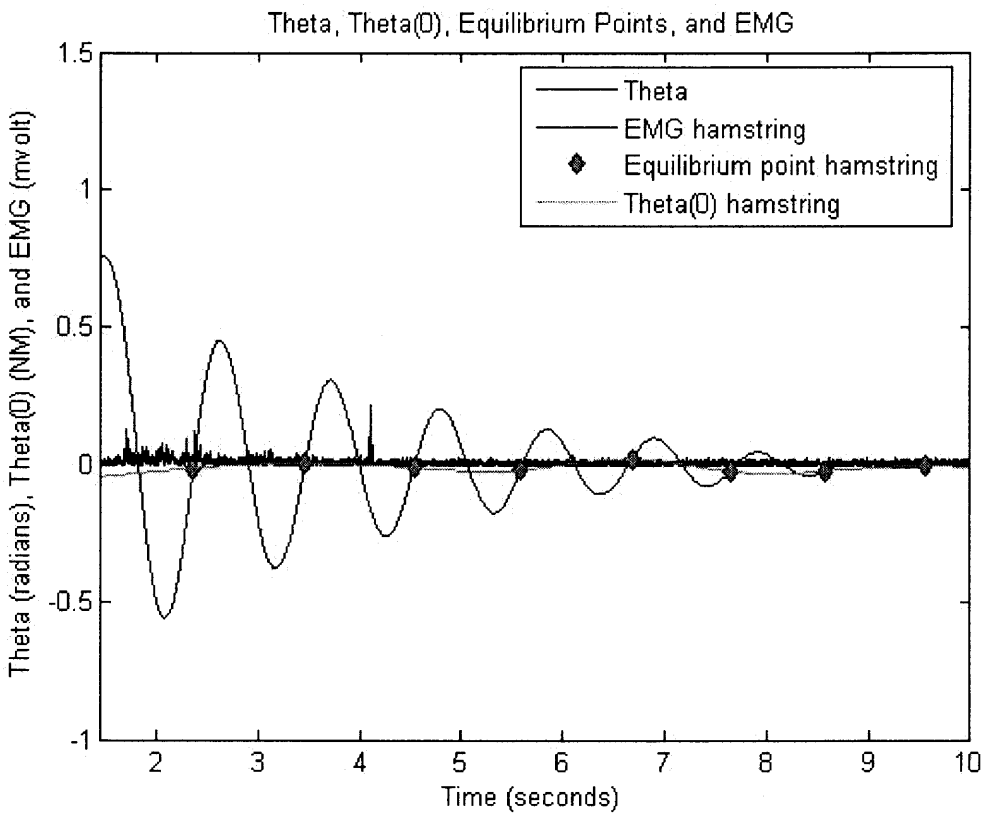

Figure 4.27: A plot of trajectory, θ, in black, EMG of the hamstring in blue, and equilibrium points and θ_0 trajectory in green.

The above graph is of the trajectory and hamstring EMG. The resultant EMG of the hamstring reveals mostly noise. Further, the equilibrium points are at or close to zero.

By the nature of surface electrodes attached to deformable skin, there exists the possibility that perceived findings are simply movement artifact or noise. This research concludes, however, that the existence of muscle activation in the early swing is possible and logical. During the first swing, the leg is moving at a velocity of 172.97 degrees/second, which is above the documented threshold of roughly 150 degrees/second to elicit muscle activation.

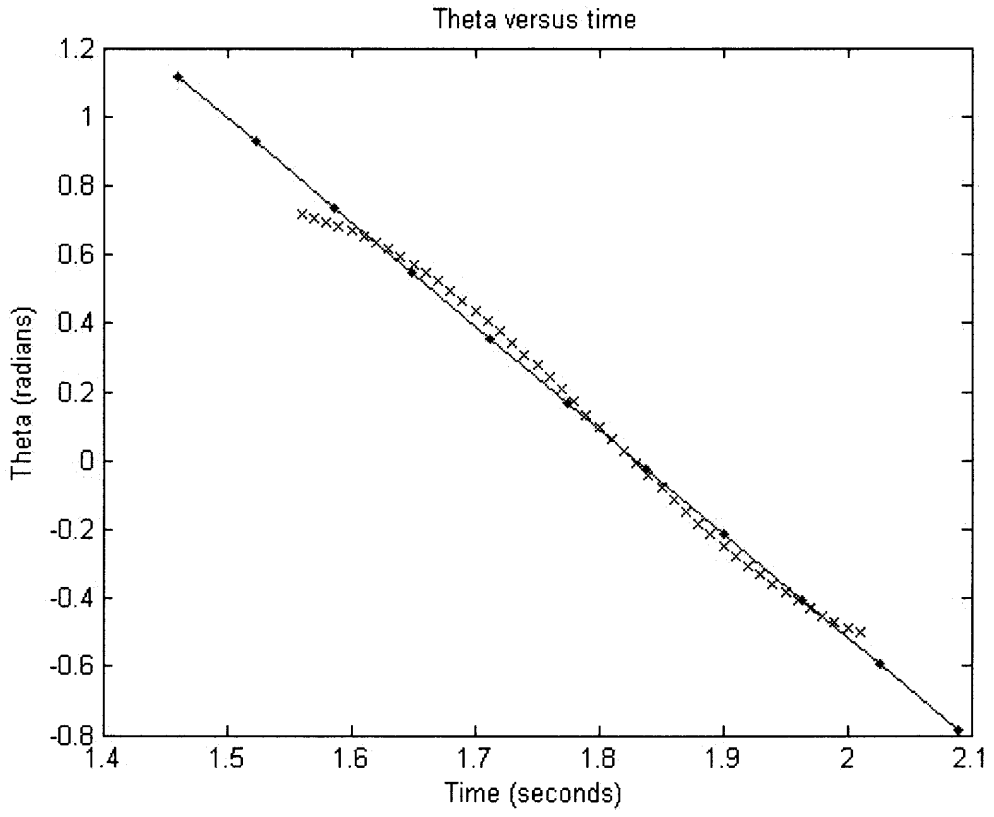

Figure 4.28: The slope of the first swing indicates velocity being 172.97 degrees/second.

In effort to further prove that the EMG is valid, it was averaged over the three trials. The following graphs indicate activity in the quadriceps in the first swing. Since this is an average, this research concludes that the existence of activity is real.

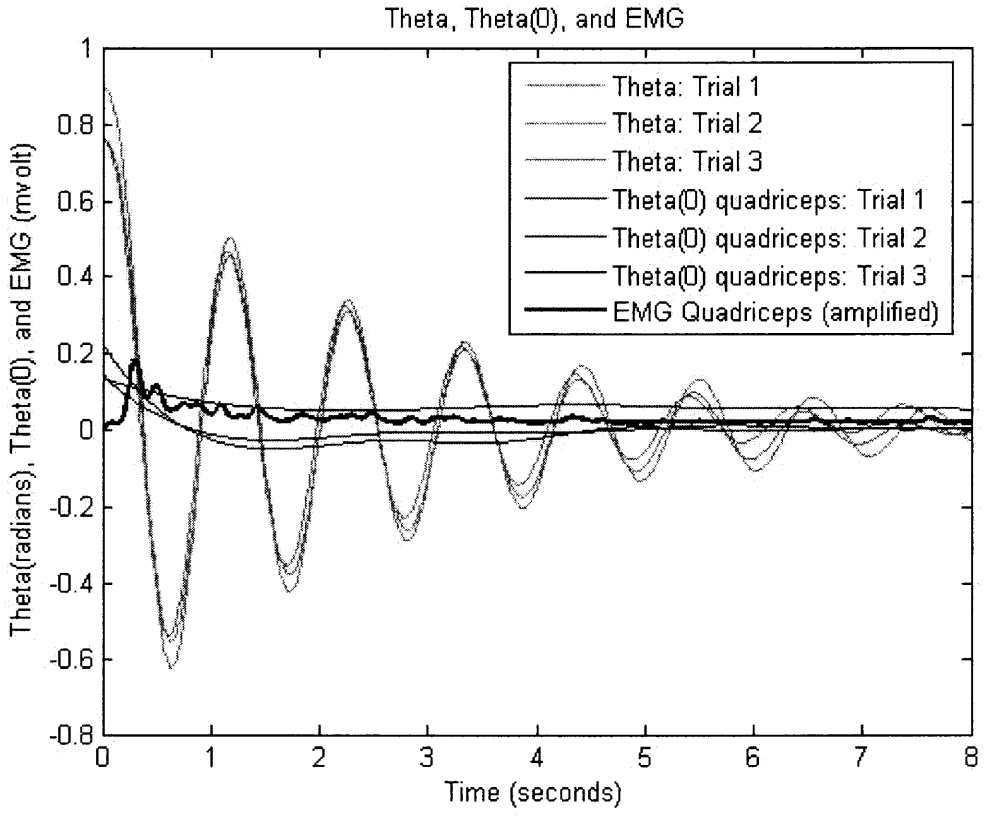

Figure 4.29: A plot of the three trajectories, θ, in green, EMG envelope of the quadriceps in blue, and θ_0 trajectories for three trials in red.

The following graph is the average EMG of the hamstring, with θ and θ_0 trajectories. This research concludes that there is little activity in the hamstring muscle during the pendulum knee drop test.

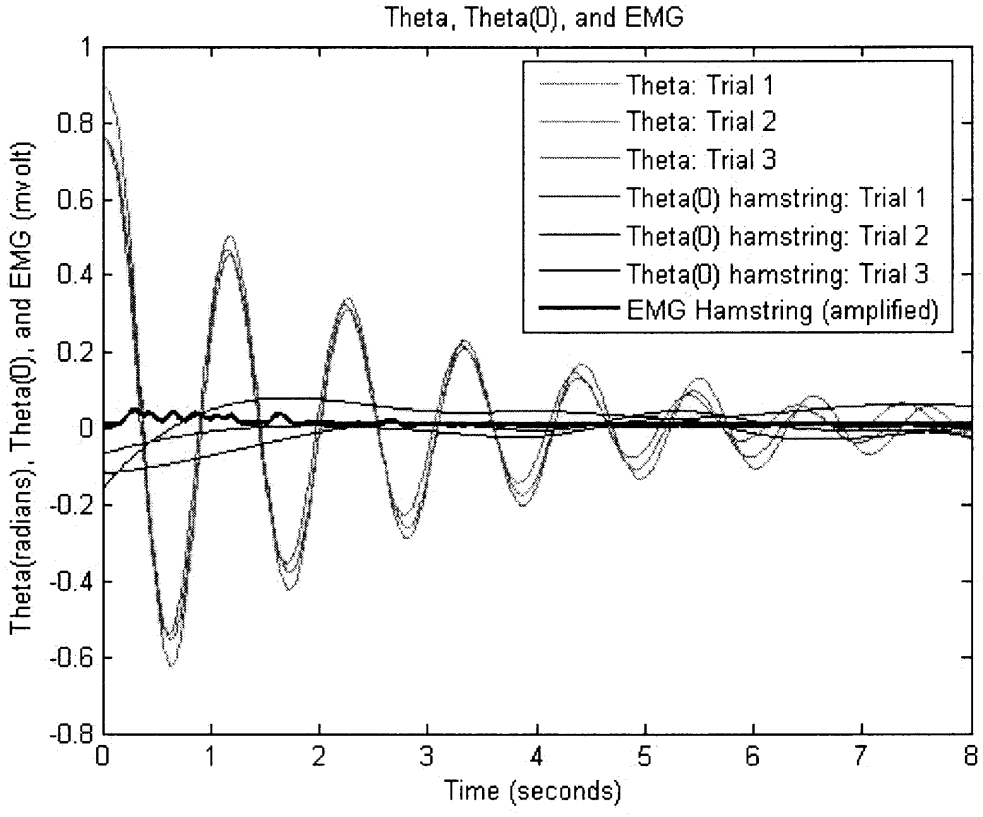

Figure 4.30: A plot of the three trajectories, θ, in green, EMG envelope of the hamstring in blue, and θ_0 trajectories for three trials in red.

The following experiment on the non-spastic female indicates that there is possible muscle activation in early swing. EMG along with non-zero equilibrium points in the quadriceps are the basis for this hypothesis. Non-linearity in early swing has been noted by various papers, discussed in the background section. This research has hypothesized a reason for this nonlinearity.

In conclusion, this inverse model highlighted three main points. Spastic residual torque is generated by a non-zero equilibrium point trajectory and is equated with the clinical concept of hyperactive stretch reflex. Spastic residual torque can be described by an increase in passive elastic stiffness and equated with the clinical concept of tone. Muscle activation is possible in early swing of the pendulum knee drop test in non-spastic subjects. This research was a preliminarily assessment which will be used in the following years on spastic and non-spastic subjects.

4.3 Future Work

This model revealed the necessity for two main changes to be immediately established. The model could be improved if the torque required to hold the leg prior to release is added. A modification of the damping coefficient making it dynamic would also be beneficial. In the less immediate future the research would be greatly improved by utilizing Haptic Master (FCS Control Systems Inc) which is able to measure force and velocity.

One idea is to add a force transducer to measure initial resistance to passive motion and a nonlinear damping coefficient. Nordmark and Andersson cite that a handheld force transducer can be used to measure initial resistance to passive motion. The next step includes implementing the force transducer to measure the torque necessary to hold the leg prior to release. Prior to the leg being released the following equation would be employed: Mh = Mr + Mg. Since there is no movement Md and Iα are zero. This will be implemented in future work. Mh = Th*l where Th represents the torque

required to hold the leg prior to releasing it to swing and *l* is the length from transducer to the knee joint. This component reveals the initial nonlinear stiffness prior to release.

Another proposal is to make damping dynamic instead of static. The hypothesis of this model assumed that since the value of damping is small compared to stiffness it should be linear, but there are biomechanical factors that can alter the coefficient making it very nonlinear. Thixotropic effects can contribute to the viscous properties. For example, Lakie suggests that there are thixotropic effects that occur from interactions between myosin cross-bridges and actin filaments. He suggests that interaction is reduced when the muscle is oscillated and that this effect could cause the abnormal acceleration in the first swing. He believes that holding the leg could allow for thixotropic effects to build causing extreme nonlinearities in accelerations, period, and damping in the first cycle. [15] The stickiness of the interactions between myosin cross-bridges and actin filaments is a viable theory that could be a contribution to the biomechanical model.

The future of this research is to minimize the unknown values. While inverse modeling has provides a framework it is not an end point, since so many calculations and assumptions have to be made. This research would benefit from new technology such as Haptic Master, which is a robotic interface that can measure velocity and force. There are various benefits to using this in modeling, one being the ability to quantify previously estimated values such moment of inertia, trajectory, and velocity.

In conclusion, this research is a preliminary assessment of modeling in non-spastic and disabled subjects. It has provided the necessary ground for future understanding of spasticity.

REFERENCES

[1] Stein RB, Zehr EP, Lebiedowska MK, Popovic DB, Scheiner A, Chizeck HJ, "Estimating Mechanical Parameters of Leg Segments in Individuals With and Without Physical Disabilities," IEEE Transactions on Rehabilitation Engineering, vol. 4, no. 3, pp. 201-11, September 1996.

[2] Burke D, Andrews CJ, Gillies JD, "The Reflex Response to Sinusoidal Stretching in Spastic Man," Brain, vol. 94 no. 3, pp. 455-70, 1971.

[3] Mirbagheri MM, Tsao C, Rymer WZ, "Abnormal Intrinsic and Reflex Stiffness Related to Impaired Voluntary Movement," 26th Annual International Conference of the IEEE EMBS, Department of Physical Medicine and Rehabilitation, September 2004.

[4] Le Cavorzin P, Poudens SA, Chagneau F, Carrault G, Allain H, Rochcongar P, "A Comprehensive Model of Spastic Hypertonia Derived from the Pendulum Test of the Leg," Muscle Nerve, vol. 24, no. 12, pp. 1612-21, December 2001.

[5] He J, Norling WR, Wang Y, "A dynamic neuromuscular model for describing the pendulum test of spasticity," IEEE Transactions on Biomedical Engineering, vol. 44, no. 3, pp. 175-84, March 1997.

[6] Schmit BD, Dhaher Y, Dewald JP, Rymer WZ, "Reflex Torque Response to Movement of the Spastic Elbow: Theoretical Analyses and Implications for Quantification of Spasticity," Annals of Biomedical Engineering, vol. 27, no. 6, pp. 815-29, Nov-Dec 1999.

[7] Nordmark E, Anderson G, "Wartenberg Pendulum Test: Objective Quantification of Muscle Tone in Children with Spastic Diplegia Undergoing Selective Dorsal Rhizotomy," Developmental Medicine and Child Neurology, vol. 44, no. 1, pp. 26-33, January 2002.

[8] Nielson JB, Petersen NT, Crone C, Sinkjaer T, "Stretch Reflex Regulation in Healthy Subjects and Patients With Spasticity," Neuromodulation, vol. 8, pp. 49-57, 2005.

[9] Fee JW Jr, Foulds RA, "Neuromuscular Modeling of Spasticity in Cerebral Palsy," IEEE Transactions on Neural Systems Rehabilitative Engineering, vol. 12 no. 1, pp. 55-64, March 2004.

[10] Winter DA, Biomechanics and Motor Control of Human Movement, New York: Wiley, 2005.

[11] Lance JW, "Pathophysiology of Spasticity and Clinical Experience with Baclofen," Spasticity: Disordered Motor Control, pp. 185-203, 1980.

[12] Mirbagheri MM, Barbeau H, Ladouceur M, Kearney RE, "Intrinsic and Reflex Stiffness in Normal and Spastic, Spinal Cord Injured Subjects," Exp Brain Res, vol. 141, no. 4, pp. 446-59, December 2001.

[13] Fowler EG, Nwigwe AI, Ho TW, "Sensitivity of the Pendulum Test for Assessing Spasticity in Persons with Cerebral Palsy," Developmental Medicine and Child Neurology, vol. 42 no. 3, pp. 182-9 March 2003.

[14] Lakie M, Walsh EG, Wright GW, "Resonance at the wrist demonstrated by the use of a torque motor: an instrumental analysis of muscle tone in man," Journal of Physiology, vol. 353, pp. 265-85, August 1984.

[15] Lin DC, Rymer WZ, "A Quantitative Analysis of Pendular Motion of the Lower Leg in Spastic Human Subjects," IEEE Transactions on Biomedical Engineering, vol. 38, no. 9, pp. 906-18, September 1991.

[16] Jobin A, Levin MF, "Regulation of Stretch Reflex Threshold in Elbow Flexors in Children with Cerebral Palsy: A New Measure of Spasticity," Developmental Medicine and Child Neurology, vol. 42, no. 8, pp. 531-40. August 2000.

[17] McFaull SR, Lamontagne M, "In Vivo Measurement of the Passive Viscoelastic Properties of the Human Knee Joint," Human Movement Science, vol. 17, pp. 139-165. 1998.

[18] Esteki A, Mansour JM, "An Experimentally Based Nonlinear Viscoelastic Model of Joint Passive Moment," Journal of Biomechanics, vol. 29, no. 4, pp. 443-50 April 1996.

[19] Lum PS, Burgar CG, Kenney DE, Van der Loos HF, "Quantification of Force Abnormalities During Passive and Active-Assisted Upper-Limb Reaching Movements in Post-Stroke Hemiparesis," IEEE Transactions on Biomedical Engineering, vol. 46, no. 6, pp. 652-62, June 1999.

[20] Hidler JM, Harvey RL, Rymer WZ, "Frequency Response Characteristics of Ankle Plantar Flexors in Humans Following Spinal Cord Injury: Relation To Degree of Spasticity," Annals of Biomedical Engineering, vol. 30, no. 7, pp. 969-81, July-August 2002.

[21] Nordez A, Cornu C, McNair P, "Acute Effects of Static Stretching on Passive Stiffness of the Hamstring Muscles Calculated Using Different Mathematical Models," Clinical Biomechanics, vol. 21, no. 7, pp. 755-60, August 2006.

[22] Leonard CT, The Neuroscience of Human Movement, Missouri: Mosbi, 1998.

[23] Shadmehr R, "The Equilibrium Point Hypothesis for Control of Movements," 1998.

[24] Weiss PL, Hunter IW, Kearney RE, "Human Ankle Joint Stiffness Over the Full Range of Muscle Activation Levels," Journal of Biomechanics, vol. 21, no. 7, pp. 539-44, 1998.

[25] Powers RK, Marder-Meyer J, Rymer WZ, "Quantitative Relations Between Hypertonia and Stretch Reflex Threshold in Spastic Hemiparesis," Annals of Neurology, vol. 23, no. 2, pp. 115-24 February 1988.

[26] Fee JW Jr, Miller F, "The Leg Drop Pendulum Test Performed Under General Anesthesia in Spastic Cerebral Palsy," Developmental Medicine and Child Neurology, vol. 46, no. 4, pp. 273-81 April 2001.

[27] Konrad P, The ABC of EMG, A Practical Introduction to Kinesiological Electromyography, vol. 1, Noraxon Inc., April 2005.